2009

Energy Decomposition Analysis of Covalent Bonds and Intermolecular Interactions

Peifeng Su
University of Nebraska - Lincoln, psu2@unl.edu

Hui Li
University of Nebraska - Lincoln, hli4@unl.edu

Energy decomposition analysis of covalent bonds and intermolecular interactions

Peifeng Su and Hui Li[a)]
Department of Chemistry, University of Nebraska-Lincoln, Nebraska 68504, USA

(Received 10 April 2009; accepted 8 June 2009; published online 2 July 2009)

An energy decomposition analysis method is implemented for the analysis of both covalent bonds and intermolecular interactions on the basis of single-determinant Hartree–Fock (HF) (restricted closed shell HF, restricted open shell HF, and unrestricted open shell HF) wavefunctions and their density functional theory analogs. For HF methods, the total interaction energy from a supermolecule calculation is decomposed into electrostatic, exchange, repulsion, and polarization terms. Dispersion energy is obtained from second-order Møller–Plesset perturbation theory and coupled-cluster methods such as CCSD and CCSD(T). Similar to the HF methods, Kohn–Sham density functional interaction energy is decomposed into electrostatic, exchange, repulsion, polarization, and dispersion terms. Tests on various systems show that this algorithm is simple and robust. Insights are provided by the energy decomposition analysis into H_2, methane C–H, and ethane C–C covalent bond formation, CH_3CH_3 internal rotation barrier, water, ammonia, ammonium, and hydrogen fluoride hydrogen bonding, van der Waals interaction, DNA base pair formation, BH_3NH_3 and BH_3CO coordinate bond formation, Cu-ligand interactions, as well as LiF, LiCl, NaF, and NaCl ionic interactions. © *2009 American Institute of Physics*.
[DOI: 10.1063/1.3159673]

I. INTRODUCTION

Intermolecular interaction plays an important role in determining the chemical and physical properties of a molecular system and has long been a focus of theoretical studies. A straightforward approach for interaction calculation is to perform a supermolecule calculation and subunit calculations with a size-consistent method and then derive the interaction energy by taking the energy difference. Accurate calculations of intermolecular interactions in some chemically interesting systems containing a few tens of atoms have been achieved by using second-order Møller–Plesset perturbation theory (MP2) and coupled-cluster singles, doubles, and noniterative triples [CCSD(T)] methods.

In addition to the knowledge of the total intermolecular interaction energy, it is often desirable to obtain the knowledge of its physical origins. This is especially useful in the development of force field methods that employ different functional forms to model interaction terms of different origins.

Intermolecular perturbation methods have been used to calculate intermolecular interactions since the beginning of quantum mechanics.[1] The symmetry-adapted perturbation theory (SAPT) method that divides the supermolecule Hamiltonian into monomer Fock operators, monomer fluctuation operators, and an interaction operator has been popularly used.[2] Recently, density functional theory based SAPT method (SAPT-DFT) was also developed.[3] Usually the SAPT interaction terms are combined and interpreted as electrostatic, exchange (or exchange-repulsion), polarization, and dispersion energies. The interaction energies obtained from supermolecule calculations with approximate (but size-consistent) methods such as Hartree–Fock (HF), MP2, and CCSD(T) are interpretable with SAPT: very similar values can be obtained by using select lower-order SAPT terms.[4] SAPT has been developed to study trimer interactions,[5] but a general extension to many-body problems is difficult.

Pioneered by studies in Refs. 6 and 7, energy decomposition analysis (EDA) methods can also provide insights into intermolecular interactions by separating the total interaction energy computed at the HF level into various terms such as electrostatic, exchange repulsion, polarization, and charge transfer. EDA methods have been extended to study many-body systems, as was done by Chen and Gordon.[8] There are many HF EDA algorithms such as the natural energy decomposition analysis (NEDA),[9] the constrained space orbital variation,[10] the reduced variational space (RVS) analysis,[8,11] the block-localized wavefunction EDA,[12] and the absolutely localized molecular orbital EDA.[13] In order to complete the interaction analysis, additional supermolecule MP2 or CCSD(T) calculations are often performed to derive the dispersion energy for these HF based methods.

EDA can also be performed for DFT methods. The extended transition state (ETS) scheme is used for bond formation and bond energy analysis within the Hartree–Fock–Slater and DFT frames: the total interaction energy is divided into electrostatic interaction, Pauli interaction, and orbital interaction energies.[14,15] Recently the NEDA and an intermolecular EDA based on fragment-localized orbitals were formulated for DFT methods.[16]

In this work, a simple, robust, and basis set insensitive EDA method is implemented. This method can be considered

[a)]Author to whom correspondence should be addressed. Electronic mail: hli4@unl.edu.

as an extension and modification of the methods developed by Kitaura and Morokuma,[7] Ziegler and Rauk,[17] and Hayes and Stone.[18] The main features of the new implementation are as follows:

(1) The electrostatic, exchange, and repulsion terms are isolated, according to Hayes and Stone's method,[18] from the Heitler–London interaction energy derived from an antisymmetric product of the monomer HF spin orbitals. In Kitaura and Morokuma's method[7] and many other methods, exchange and repulsion are not separated. In some other methods, the Heitler–London term is not separated at all. Formulated with spin orbitals, the new implementation can deal with both closed and open shell systems described by single-determinant restricted closed shell Hartree–Fock (RHF), restricted open shell Hartree–Fock (ROHF), and unrestricted open shell Hartre–Fock (UHF) wavefunctions and, therefore, can analyze both covalent bonds and intermolecular interactions.
(2) The polarization energy is defined as the "orbital relaxation energy" on going from the monomer HF spin orbitals to the supermolecule HF spin orbitals, conceptually similar to the "electronic interaction energy" defined for the Hartree–Fock–Slater method by Ziegler and Rauk.[17] This variational HF polarization energy is different from the perturbational polarization energy derived from SAPT, in which polarization and dispersion energies arise together at the second and higher orders of perturbation.
(3) The dispersion energy is derived via a supermolecule approach using size-consistent correlation methods such as MP2 and CCSD(T). This has been a standard practice in the literature.
(4) For Kohn–Sham (KS) DFT methods, the total KS interaction energy is decomposed into electrostatic, exchange, repulsion, polarization, and dispersion terms. The exchange and dispersion terms are defined using the changes in the exchange and correlation functionals on going from monomers to supermolecule.

The intermolecular interaction analysis discussed in the current paper is not dependent on or related to the choice of canonical or localized or any other type of molecular orbitals. In Sec. II below, the details of this method are described.

II. THEORY

A. Hartree–Fock interaction

In this subsection the decomposition of the HF interaction energy is described. As mentioned in Sec. I, the separation of the Heitler–London term is identical to those used by Hayes and Stone.[18] It is necessary to introduce these equations here in order to derive similar equations for the KS method in Sec. II B.

Using a single-determinant wavefunction Φ to approximate the true wavefunction, the HF energy E^{HF} is obtained:

$$E^{\mathrm{HF}} = \langle \Phi | H | \Phi \rangle, \tag{1}$$

where H is the Hamiltonian and Φ is formed by a set of molecular orbitals that variationally minimizes the E^{HF}. These orbitals are the HF orbitals and are usually expanded in a set of basis functions.

If the molecular HF spin orbitals are orthonormal to each other, the corresponding energy E^{HF} can be written as the orbital energy integrals:

$$E^{\mathrm{HF}} = \sum_{i}^{\alpha,\beta} h_i + \frac{1}{2}\sum_{i}^{\alpha,\beta}\sum_{j}^{\alpha,\beta} \langle ii|jj\rangle - \frac{1}{2}\sum_{i}^{\alpha}\sum_{j}^{\alpha} \langle ij|ij\rangle - \frac{1}{2}\sum_{i}^{\beta}\sum_{j}^{\beta} \langle ij|ij\rangle + E^{\mathrm{nuc}}, \tag{2}$$

where i and j run over the occupied α and β spin orbitals or both, h_{ik} and $\langle ii|jj\rangle$ and $\langle ij|ij\rangle$ are one-electron and two-electron Coulomb and exchange integrals, and E^{nuc} is the nuclear repulsion energy.

It is not necessary for the molecular orbitals to be orthonormal to each other in order to minimize E^{HF}. For example, once a set of orthonormal HF orbitals is obtained, any linear combination of the occupied HF orbitals, even nonorthonormal, still produces the same E^{HF} because they result in the same determinant Φ in Eq. (1). In general, if a set of nonorthonormal orbitals is used to represent the HF orbitals, the E^{HF} can be written as

$$E^{\mathrm{HF}} = \sum_{i}^{\alpha,\beta}\sum_{j}^{\alpha,\beta} h_{ij}(S^{-1})_{ij} + \frac{1}{2}\sum_{i}^{\alpha,\beta}\sum_{j}^{\alpha,\beta}\sum_{k}^{\alpha,\beta}\sum_{l}^{\alpha,\beta} \langle ij|kl\rangle \times (S^{-1})_{ij}(S^{-1})_{kl} - \frac{1}{2}\sum_{i}^{\alpha}\sum_{j}^{\alpha}\sum_{k}^{\alpha}\sum_{l}^{\alpha} \langle ik|jl\rangle \times (S^{-1})_{ij}(S^{-1})_{kl} - \frac{1}{2}\sum_{i}^{\beta}\sum_{j}^{\beta}\sum_{k}^{\beta}\sum_{l}^{\beta} \langle ik|jl\rangle \times (S^{-1})_{ij}(S^{-1})_{kl} + E^{\mathrm{nuc}}, \tag{3}$$

where i, j, k, and l run over occupied α and β spin orbitals or both and h_{ik} and $\langle ij|kl\rangle$ and $\langle ik|jl\rangle$ are one- and two-electron integrals. S^{-1} is the inverse of the overlap matrix S of the spin orbitals. For two orbitals with opposite spins, their overlap integral is simply zero. Only for two like-spin orbitals can their overlap be possibly nonzero. If the alpha and beta-spin orbitals are grouped together, the S matrix is block diagonal, and so is the S^{-1} matrix.

For a supermolecule X consisting of monomers A, the total HF interaction energy is

$$\Delta E^{\mathrm{HF}} = \langle \Phi_X | H_X | \Phi_X \rangle - \sum_{A} \langle \Phi_A | H_A | \Phi_A \rangle, \tag{4}$$

where Φ_X and Φ_A are the variational single-determinant HF wavefunctions for the supermolecule X and a monomer A. In the following it is shown that using various approximate HF energy expressions for the supermolecule, the total HF interaction energy ΔE^{HF} can be decomposed into electrostatic, exchange, repulsion, and polarization terms:

$$\Delta E^{\mathrm{HF}} = \Delta E^{\mathrm{ele}} + \Delta E^{\mathrm{ex}} + \Delta E^{\mathrm{rep}} + \Delta E^{\mathrm{pol}}. \tag{5}$$

The electrostatic energy can be obtained by using the following approximate energy expression for a supermolecule X consisting of monomers A:

$$E_X^{(1)} = \sum_{i\in X}^{\alpha,\beta} h_i + \frac{1}{2}\sum_{i\in X}^{\alpha,\beta}\sum_{j\in X}^{\alpha,\beta}\langle ii|jj\rangle - \sum_A \left(\frac{1}{2}\sum_{i\in A}^{\alpha}\sum_{j\in A}^{\alpha}\langle ij|ij\rangle + \frac{1}{2}\sum_{i\in A}^{\beta}\sum_{j\in A}^{\beta}\langle ij|ij\rangle\right) + E_X^{\mathrm{nuc}}. \tag{6}$$

The spin orbitals i and j are the variationally optimized HF orbitals that minimize the HF energy of each monomer and are orthonormal to each other within each monomer. They are not variationally optimized to minimize the supermolecule HF energy and are not necessarily orthonormal to each other between the monomers. Compared to Eq. (2), the $E_X^{(1)}$ in Eq. (6) does not contain the exchange term between the monomers.

The electrostatic interaction energy between the monomers A in a supermolecule X is

$$\Delta E^{\mathrm{ele}} = E_X^{(1)} - \sum_A E_A^{\mathrm{HF}} = \frac{1}{2}\sum_{i\in X}^{\alpha,\beta}\sum_{j\in X}^{\alpha,\beta}\langle ii|jj\rangle + E_X^{\mathrm{nuc}} - \sum_A \left(\frac{1}{2}\sum_{i\in A}^{\alpha,\beta}\sum_{j\in A}^{\alpha,\beta}\langle ii|jj\rangle + E_A^{\mathrm{nuc}}\right). \tag{7}$$

For RHF cases, the ΔE^{ele} defined in Eq. (7) is the same as in the Kitaura–Morokuma EDA and is additive for a supermolecule consisting of many monomers.

The exchange energy can be obtained by using the following approximate energy expressions for the supermolecule X:

$$E_X^{(2)} = \sum_{i\in X}^{\alpha,\beta} h_i + \frac{1}{2}\sum_{i\in X}^{\alpha,\beta}\sum_{j\in X}^{\alpha,\beta}\langle ii|jj\rangle - \frac{1}{2}\sum_{i\in X}^{\alpha}\sum_{j\in X}^{\alpha}\langle ij|ij\rangle - \frac{1}{2}\sum_{i\in X}^{\beta}\sum_{j\in X}^{\beta}\langle ij|ij\rangle + E_X^{\mathrm{nuc}}. \tag{8}$$

Again, the spin orbitals i and j are the orthonormal HF spin orbitals of the monomers and are not necessarily orthonormal to each other between the monomers. Compared to Eq. (6), Eq. (8) contains the exchange terms between the monomers and has the same form as Eq. (2).

The exchange energy is defined as

$$\Delta E^{\mathrm{ex}} = E_X^{(2)} - E_X^{(1)} = -\frac{1}{2}\sum_{i\in X}^{\alpha}\sum_{j\in X}^{\alpha}\langle ij|ij\rangle - \frac{1}{2}\sum_{i\in X}^{\beta}\sum_{j\in X}^{\beta}\langle ij|ij\rangle - \sum_A \left(\frac{1}{2}\sum_{i\in A}^{\alpha}\sum_{j\in A}^{\alpha}\langle ij|ij\rangle - \frac{1}{2}\sum_{i\in A}^{\beta}\sum_{j\in A}^{\beta}\langle ij|ij\rangle\right). \tag{9}$$

The exchange energy defined in Eq. (9) is additive for a supermolecule consisting of many monomers.

The following approximate energy expression for the supermolecule can be obtained if the monomer orbitals are used to form a single-determinant wavefunction [note that the orbital orthonormality is enforced by S^{-1} as shown in Eq. (3)]:

$$E_X^{(3)} = \sum_{i\in X}^{\alpha,\beta}\sum_{j\in X}^{\alpha,\beta} h_{ij}(S^{-1})_{ij} + \frac{1}{2}\sum_{i\in X}^{\alpha,\beta}\sum_{j\in X}^{\alpha,\beta}\sum_{k\in X}^{\alpha,\beta}\sum_{l\in X}^{\alpha,\beta}\langle ij|kl\rangle \times (S^{-1})_{ij}(S^{-1})_{kl} - \frac{1}{2}\sum_{i\in X}^{\alpha}\sum_{j\in X}^{\alpha}\sum_{k\in X}^{\alpha}\sum_{l\in X}^{\alpha}\langle ik|jl\rangle \times (S^{-1})_{ij}(S^{-1})_{kl} - \frac{1}{2}\sum_{i\in X}^{\beta}\sum_{j\in X}^{\beta}\sum_{k\in X}^{\beta}\sum_{l\in X}^{\beta}\langle ik|jl\rangle \times (S^{-1})_{ij}(S^{-1})_{kl} + E_X^{\mathrm{nuc}}. \tag{10}$$

Again, i, j, k, and l are the orthonormal HF spin orbitals of the monomers and are not necessarily orthonormal to each other between the monomers; S^{-1} is the inverse of the overlap matrix S of all of the monomer spin orbitals. Because the monomer spin orbitals are not necessarily orthonormal to each other between the monomers, the S and S^{-1} matrices are not unit matrices.

The repulsion energy is defined as

$$\Delta E^{\mathrm{rep}} = E_X^{(3)} - E_X^{(2)}. \tag{11}$$

For RHF cases, the sum of the ΔE^{ex} and ΔE^{rep} defined in Eqs. (9) and (11) is the same as the exchange-repulsion term in the Kitaura–Morokuma EDA. Because Eq. (10) enforces the simultaneous orthonormalization of all the orbitals from all monomers (by using the inverse of the supermolecule overlap matrix S), the repulsion energy is not pairwise additive for a supermolecule consisting of many monomers.

For a supermolecule X consisting of monomers A, the HF polarization interaction energy is defined as

$$\Delta E^{\mathrm{pol}} = E_X^{\mathrm{HF}} - E_X^{(3)}, \tag{12}$$

where E_X^{HF} is the HF energy of the supermolecule X. For RHF cases, the ΔE^{pol} defined by Eq. (12) is equivalent to the sum of the polarization, the charge transfer, and the mixing term in the Kitaura–Morokuma EDA. For a supermolecule consisting of many monomers, the ΔE^{pol} is not additive.

For MP2, CCSD, and CCSD(T) methods that use single-determinant HF wavefunctions as references, the total interaction energy can be naturally separated into HF interaction and dispersion interaction. For example, in the CCSD(T) case,

$$\Delta E^{\mathrm{CCSD(T)}} = \Delta E^{\mathrm{HF}} + \Delta E^{\mathrm{disp}} = \Delta E^{\mathrm{HF}} + (\Delta E^{\mathrm{CCSD(T)}} - \Delta E^{\mathrm{HF}}), \tag{13}$$

where the dispersion term ΔE^{disp} is simply the difference between the CCSD(T) and HF interaction energies. Apparently, the interaction energy terms defined by Eqs. (7), (9), and (11)–(13) are valid for the RHF, ROHF, and UHF methods.

B. Kohn–Sham method

Similar to the HF method, using a single-determinant wavefunction Φ formed by a set of orthonormal orbitals, the KS energy E^{KS} can be written as [see Eq. (2)]

$$E^{\mathrm{KS}} = \sum_{i}^{\alpha,\beta} h_i + \frac{1}{2}\sum_{i}^{\alpha,\beta}\sum_{j}^{\alpha,\beta} \langle ii|jj\rangle + E_x[\rho^\alpha,\rho^\beta] + E_c[\rho^\alpha,\rho^\beta] + E^{\mathrm{nuc}}, \tag{14}$$

where h_i and $\langle ii|jj\rangle$ are the one- and two-electron integrals and E^{nuc} is the nuclear repulsion energy, $E_x[\rho^\alpha,\rho^\beta]$ and $E_c[\rho^\alpha,\rho^\beta]$ are the exchange and correlation functionals, and ρ^α and ρ^β are the alpha-spin and beta-spin electron density functions, which are the sum of the square of each occupied KS spin orbital (assume orthonormal real functions):

$$\rho^\alpha = \sum_{i}^{\alpha} \psi_i\psi_i, \qquad \rho^\beta = \sum_{i}^{\beta} \psi_i\psi_i. \tag{15}$$

Similar to the HF methods, it is not necessary for the KS orbitals to be orthonormal to each other in order to minimize E^{KS}. In general, if a set of nonorthonormal orbitals is used the E^{KS} can be written as

$$E^{\mathrm{KS}} = \sum_{i}^{\alpha,\beta}\sum_{j}^{\alpha,\beta} h_{ij}(S^{-1})_{ij} + \frac{1}{2}\sum_{i}^{\alpha,\beta}\sum_{j}^{\alpha,\beta}\sum_{k}^{\alpha,\beta}\sum_{l}^{\alpha,\beta} \langle ij|kl\rangle \times (S^{-1})_{ij}(S^{-1})_{kl} + E_x[\rho^\alpha,\rho^\beta] + E_c[\rho^\alpha,\rho^\beta] + E^{\mathrm{nuc}}. \tag{16}$$

The summations in Eq. (16) are over occupied α and β spin orbitals or both; h_{ik} and $\langle ik|rs\rangle$ are one- and two-electron integrals. The electron density functions ρ^α and ρ^β in Eq. (16) must be rewritten as

$$\rho^\alpha = \sum_{i}^{\alpha}\sum_{j}^{\alpha} \psi_i\psi_j(S^{-1})_{ij}, \qquad \rho^\beta = \sum_{i}^{\beta}\sum_{j}^{\beta} \psi_i\psi_j(S^{-1})_{ij}. \tag{17}$$

It is trivial to show that the density functions in Eq. (17) are the same as those in Eq. (15) as long as the nonorthonormal orbitals give the same E^{KS}. Therefore, the exchange and correlation functionals remain unchanged on going from orthornormal to nonorthonormal representations of the KS orbitals.

For a supermolecule X consisting of monomers A, the total KS interaction energy is

$$\Delta E^{\mathrm{KS}} = E_X^{\mathrm{KS}} - \sum_A E_A^{\mathrm{KS}}. \tag{18}$$

In principle, if the exact exchange-correlation functionals are known, Eq. (18) gives the true interaction energy.

In the following it is shown that the total KS interaction energy ΔE^{KS} can be decomposed into electrostatic, exchange, repulsion, polarization, and dispersion terms:

$$\Delta E^{\mathrm{KS}} = \Delta E^{\mathrm{ele}} + \Delta E^{\mathrm{ex}} + \Delta E^{\mathrm{rep}} + \Delta E^{\mathrm{pol}} + \Delta E^{\mathrm{disp}}. \tag{19}$$

The electrostatic energy can be obtained by using the following approximate energy expressions for the supermolecule X:

$$E_X^{(1)} = \sum_{i\in X}^{\alpha,\beta} h_i + \frac{1}{2}\sum_{i\in X}^{\alpha,\beta}\sum_{j\in X}^{\alpha,\beta} \langle ii|jj\rangle + \sum_A E_x[\rho_A^\alpha,\rho_A^\beta] + \sum_A E_c[\rho_A^\alpha,\rho_A^\beta] + E_X^{\mathrm{nuc}}. \tag{20}$$

The spin orbitals i and j are the variationally optimized KS orbitals that minimize the KS energy of each monomer and are orthonormal to each other within each monomer. They are not variationally optimized to minimize the supermolecule KS energy and are not necessarily orthonormal to each other between the monomers. The exchange and correlation functionals are simply the sums of the monomer values.

The KS electrostatic interaction energy is defined as

$$\Delta E^{\mathrm{ele}} = E_X^{(1)} - \sum_A E_A^{\mathrm{KS}} = \frac{1}{2}\sum_{i\in X}^{\alpha,\beta}\sum_{j\in X}^{\alpha,\beta} \langle ii|jj\rangle + E_X^{\mathrm{nuc}} - \sum_A \left(\frac{1}{2}\sum_{i\in A}^{\alpha,\beta}\sum_{j\in A}^{\alpha,\beta} \langle ii|jj\rangle + E_A^{\mathrm{nuc}}\right). \tag{21}$$

The KS exchange energy can be obtained by using the following approximate energy expression for the supermolecule X:

$$E_X^{(2)} = \sum_{i\in X}^{\alpha,\beta} h_i + \frac{1}{2}\sum_{i\in X}^{\alpha,\beta}\sum_{j\in X}^{\alpha,\beta} \langle ii|jj\rangle + E_x\left[\sum_A \rho_A^\alpha, \sum_A \rho_A^\beta\right] + \sum_A E_c[\rho_A^\alpha,\rho_A^\beta] + E_X^{\mathrm{nuc}}. \tag{22}$$

Again, i and j are the variationally determined KS spin orbitals for the monomers and are not necessarily orthonormal to each other between the monomers.

The KS exchange interaction is defined as

$$\Delta E^{\mathrm{ex}} = E_X^{(2)} - E_X^{(1)} = E_x\left[\sum_A \rho_A^\alpha, \sum_A \rho_A^\beta\right] - \sum_A E_x[\rho_A^\alpha,\rho_A^\beta]. \tag{23}$$

In general, since the exchange functional $E_x[\rho]$ is nonlinear, ΔE^{ex} is not zero.

The KS repulsion energy can be obtained by using the following approximate energy expression for the supermolecule X:

$$E_X^{(3)} = \sum_{i\in X}^{\alpha,\beta}\sum_{j\in X}^{\alpha,\beta} h_{ij}(S^{-1})_{ij} + \frac{1}{2}\sum_{i\in X}^{\alpha,\beta}\sum_{j\in X}^{\alpha,\beta}\sum_{k\in X}^{\alpha,\beta}\sum_{l\in X}^{\alpha,\beta} \langle ij|kl\rangle \times (S^{-1})_{ij}(S^{-1})_{kl} + E_x[\rho_X^{\alpha*},\rho_X^{\beta*}] + \sum_A E_c[\rho_A^\alpha,\rho_A^\beta] + E_X^{\mathrm{nuc}}. \tag{24}$$

Again, i, j, k, and l are the variationally determined KS spin orbitals for the monomers and are not necessarily orthonormal to each other between the monomers. Therefore, the S and S^{-1} matrices are not unit matrices. The $\rho_X^{\alpha*}$ and $\rho_X^{\beta*}$ in Eq. (24) are the alpha-spin and beta-spin electron density functions calculated using the orthonormalized monomer KS spin orbitals:

$$\rho_X^{\alpha*} = \sum_{i\in X}^{\alpha}\sum_{j\in X}^{\alpha} \psi_i\psi_j(S^{-1})_{ij},$$
$$\rho_X^{\beta*} = \sum_{i\in X}^{\beta}\sum_{j\in X}^{\beta} \psi_i\psi_j(S^{-1})_{ij}. \tag{25}$$

Since S and S^{-1} are not unit matrices, $\rho_X^{\alpha*}$ and $\rho_X^{\beta*}$ for the supermolecule are not the respective sums of the monomer density functions:

$$\rho_X^{\alpha*} \neq \sum_A \rho_A^{\alpha},$$
$$\rho_X^{\beta*} \neq \sum_A \rho_A^{\beta}. \tag{26}$$

Clearly, the three exchange functionals appearing in Eqs. (23) and (24) are different:

$$E_x[\rho_X^{\alpha*},\rho_X^{\beta*}] \neq E_x\left[\sum_A \rho_A^{\alpha},\sum_A \rho_A^{\beta}\right] \neq \sum_A E_x[\rho_A^{\alpha},\rho_A^{\beta}]. \tag{27}$$

The KS repulsion energy is defined as

$$\Delta E^{\mathrm{rep}} = E_X^{(3)} - E_X^{(2)}. \tag{28}$$

The KS polarization energy can be obtained by using the following approximate energy expression for the supermolecule X:

$$\begin{aligned} E_X^{(4)} &= \sum_{i\in X}^{\alpha,\beta}\sum_{j\in X}^{\alpha,\beta} h_{ij}(S^{-1})_{ij} + \frac{1}{2}\sum_{i\in X}^{\alpha,\beta}\sum_{j\in X}^{\alpha,\beta}\sum_{k\in X}^{\alpha,\beta}\sum_{l\in X}^{\alpha,\beta}\langle ij|kl\rangle \\ &\quad\times(S^{-1})_{ij}(S^{-1})_{kl} + E_x[\rho_X^{\alpha},\rho_X^{\beta}] + \sum_A E_c[\rho_A^{\alpha},\rho_A^{\beta}] + E_X^{\mathrm{nuc}} \\ &= \sum_{i\in X}^{\alpha,\beta} h_i + \frac{1}{2}\sum_{i\in X}^{\alpha,\beta}\sum_{j\in X}^{\alpha,\beta}\langle ii|jj\rangle + E_x[\rho_X^{\alpha},\rho_X^{\beta}] \\ &\quad + \sum_A E_c[\rho_A^{\alpha},\rho_A^{\beta}] + E_X^{\mathrm{nuc}}, \end{aligned} \tag{29}$$

where i, j, k, and l are the variationally determined orthonormal KS spin orbitals for the supermolecule X and S^{-1} is a unit matrix.

The KS polarization energy is defined as

$$\Delta E^{\mathrm{pol}} = E_X^{(4)} - E_X^{(3)}. \tag{30}$$

Finally, the KS dispersion energy is defined as

$$\Delta E^{\mathrm{disp}} = E_X^{\mathrm{KS}} - E_X^{(4)} = E_c[\rho_X^{\alpha},\rho_X^{\beta}] - \sum_A E_c[\rho_A^{\alpha},\rho_A^{\beta}], \tag{31}$$

where ρ_X^{α} and ρ_X^{β} are the supermolecular electron densities that minimize the KS energy of the supermolecule and ρ_A^{α} and ρ_A^{β} are the monomer electron density functions that minimize the KS energy of each monomer. Apparently, Eqs. (21), (23), (28), (30), and (31) are valid for the R-KS, RO-KS, and U-KS methods.

III. IMPLEMENTATION AND COMPUTATIONAL METHODS

All calculations were performed with the quantum chemistry program package GAMESS,[19] in which the EDA method was implemented by the authors. The EDA program uses existing programs in GAMESS to perform RHF, ROHF, and UHF (and their DFT analogs) self-consistent field (SCF) calculations. MP2, CCSD, and CCSD(T) energy calculations using RHF, ROHF, and UHF references were also interfaced with the method. Most of these calculations, especially the MP2,[20] CCSD, and CCSD(T) ones,[21] have been parallelized in GAMESS in previous work (by other authors) using the distributed data interface.[22] However, it is noted that currently RO-CCSD is not parallelized, and CCSD/UHF is not available. The EDA calculation is always affordable as long as the supermolecule calculation is affordable at the requested level of theory, with a computing time that is two to three times longer due to the interaction analysis which involves integral transformations from the basis set to the molecular orbitals. The largest calculation that occurred in this work is the MP2/aug-cc-pVQZ calculations for a DNA base pair (30 atoms and 2600 basis functions), which took 14 days on a four-node 32-processor 128 Gbyte random access memory cluster.

The counterpoise (CP) method proposed by Boys and Bernardi[23] for correcting the basis set superposition error (BSSE) is implemented as an option so the monomers can use the supermolecule basis set. Usually HF and MP2 calculations with the supermolecule basis set are not problematic, but DFT-SCF and CCSD iterations are sometimes divergent when the supermolecule basis set is used. Most of the calculations performed in this work used the BSSE correction.

A flow chart of the current EDA method is given in Fig. 1. The program first calculates the monomer and supermolecule HF or KS orbitals and energies at the requested level of theory. For monomers, the monomer basis sets and, optionally, the supermolecule basis set are used. If MP2 or CC calculations are requested, they will be performed immediately after the HF SCF procedure. Then it determines the intermolecular HF electrostatic and exchange interactions by virtually calculating the intermolecular Coulomb $\langle ii|jj\rangle$ and exchange $\langle ij|ij\rangle$ integrals using the monomer HF spin orbitals. This requires an integral transformation from basis functions to molecular spin orbitals. Next, the program orthornormalizes the occupied HF spin orbitals of the monomers using the S^{-1} matrix and then calculates an energy, which is used to derive the HF repulsion energy. DFT interaction energies are determined in a similar manner. Finally, the interaction terms are organized and printed out.

The aug-cc-pVnZ (n=D, T, Q, and 5) basis sets[24] were used. They are denoted as ACCD, ACCT, ACCQ, and ACC5 in the following discussions. If the CP method is used the basis sets are denoted as ACCD(CP), ACCT(CP), ACCQ(CP), and ACC5(CP). Normally this series of basis sets is used as pure spherical harmonics, but in this work all the components were used except for a few cases specially indicated in Sec. IV. The h-type functions in the ACC5 basis set are not used due to the absence of the corresponding integral

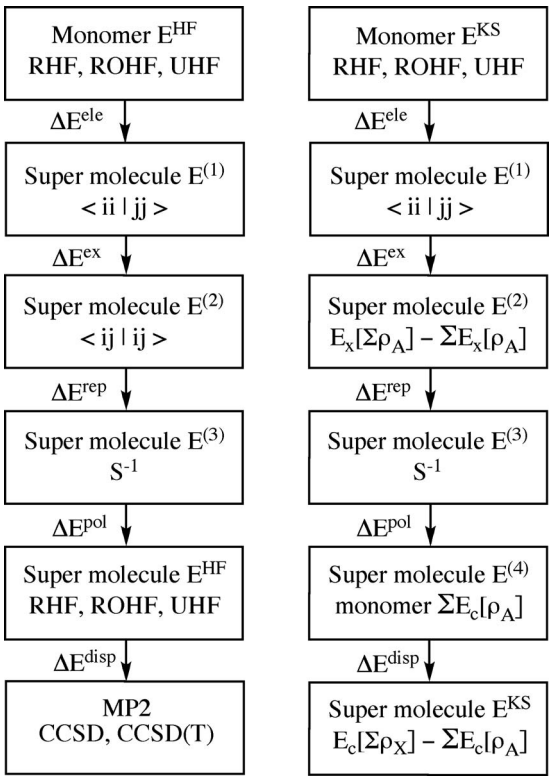

FIG. 1. Scheme of the EDA method.

codes in GAMESS. In addition, due to the linear dependences in the large basis sets, the variational space will be automatically reduced to enhance numerical stabilities in the calculations. These will usually affect the final interaction energy by a presumably very small but unknown value. For most of the cases the MP2/ACCQ method was used to optimize the supermolecular geometry. For some large systems only the ACCT or ACCD basis sets were used. It is well known that switching from ACCT to ACCQ leads to essentially no geometric changes. Compared to ACCT and ACCQ, ACCD may produce slightly different geometries but in general the results are similar.

Two DFT methods, B3LYP (Ref. 25) and BLYP,[26] were used to perform the EDA calculations in this work. All DFT methods implemented in GAMESS can be used. UHF, U-B3LYP, and U-BLYP calculations involved in this work were examined and no significant spin contaminations were found.

In this work the interaction energy between the "monomers in the supermolecule," i.e., the negative value of the equilibrium dissociation energy D_e, is discussed. Therefore, the reference for the interaction energy is the monomers that have already assumed their geometries in the supermolecule. The geometry distortion or preparation energy, zero point energy, and thermal energy are not included.

IV. RESULTS AND DISCUSSION

A. Covalent bond analysis

1. H–H

As the simplest neutral molecule, H_2 is used to illustrate the application of the current EDA method for bonding interaction analysis. The experimental H_2 bond length of 0.7413 Å is used.[27] The total interaction energy computed with CCSD/ACCQ(CP) method for H_2 is −109.21 kcal/mol

TABLE I. Covalent bond interaction analysis (kcal/mol).

Molecule	Level of theory	ΔE^{ele}	ΔE^{ex}	ΔE^{rep}	ΔE^{pol}	ΔE^{disp}	ΔE
H–H	CCSD/ACCQ(CP)//0.7413 Å	−1.47	0.00	0.00	−82.35	−25.38	−109.21
CH_3–H	RO-CCSD/ACCQ(CP)//MP2/ACCQ	−63.59	−77.47	160.66	−113.61	−23.83	−117.83
	ROMP2/ACCQ(CP)//MP2/ACCQ	−63.59	−77.47	160.66	−113.61	−24.74	−118.74
	RO-B3LYP/ACCQ(CP)//MP2/ACCQ	−60.41	−36.41	126.69	−124.82	−23.82	−118.78
	RO-BLYP/ACCQ(CP)//MP2/ACCQ	−59.31	−23.09	114.93	−126.68	−23.48	−117.64
BH_3–NH_3	CCSD(T)/ACCQ(CP)//MP2/ACCQ	−82.02	−123.58	238.65	−68.10	−9.11	−44.16
	MP2/ACCQ(CP)//MP2/ACCQ	−82.02	−123.58	238.65	−68.10	−10.02	−45.07
	B3LYP/ACCQ(CP)//MP2/ACCQ	−79.92	−53.82	178.80	−76.66	−10.06	−41.65
	BLYP/ACCQ(CP)//MP2/ACCQ	−79.76	−32.72	162.71	−78.86	−11.18	−39.82
BH_3–CO	CCSD(T)/ACCQ(CP)//MP2/ACCQ	−70.56	−154.03	303.26	−98.59	−15.91	−35.83
	MP2/ACCQ(CP)//MP2/ACCQ	−70.56	−154.03	303.26	−98.59	−18.36	−38.28
	B3LYP/ACCQ(CP)//MP2/ACCQ	−68.46	−65.32	221.78	−115.76	−12.04	−39.80
	BLYP/ACCQ(CP)//MP2/ACCQ	−68.37	−39.66	200.78	−120.70	−13.43	−41.38
CH_3–CH_3 staggered	RO-CCSD/ACCQ(CP)//MP2/ACCQ	−147.85	−191.13	400.75	−148.84	−24.77[a]	−111.69[a]
	ROMP2/ACCQ(CP)//MP2/ACCQ	−147.85	−191.13	400.75	−148.84	−31.82	−118.88
	UMP2/ACCQ(CP)//MP2/ACCQ	−145.08	−183.45	388.96	−143.63	−34.69	−117.89
	RO-B3LYP/ACCQ(CP)//MP2/ACCQ	−137.30	−82.61	298.17	−166.24	−23.06	−111.04
	RO-BLYP/ACCQ(CP)//MP2/ACCQ	−136.31	−51.35	271.38	−169.26	−24.07	−109.61
CH_3–CH_3 eclipsed	RO-CCSD/ACCQ(CP)	−148.11	−193.81	406.64	−148.56	−25.09[b]	−108.77[b]
	ROMP2/ACCQ(CP)	−148.11	−193.81	406.64	−148.56	−32.07	−115.90
	UMP2/ACCQ(CP)	−145.35	−186.14	394.87	−143.35	−34.94	−114.91
	RO-B3LYP/ACCQ(CP)	−137.59	−83.36	301.68	−165.75	−23.18	−108.20
	RO-BLYP/ACCQ(CP)	−136.61	−51.68	274.37	−168.70	−24.19	−106.81

[a]ΔE^{disp} is the CCSD(T)/ACCT(CP) value corrected by −1.68 kcal/mol from ROMP2/ACCT(CP) to ROMP2/ACCQ(CP).
[b]ΔE^{disp} is the CCSD(T)/ACCT(CP) value corrected by −1.73 kcal/mol from ROMP2/ACCT(CP) to ROMP2/ACCQ(CP).

(Table I), as compared to the experimental $-D_e$ value of −109.5 kcal/mol.[27] The electrostatic interaction energy ΔE^{ele} between two H atoms is −1.47 kcal/mol. This small attraction is caused by the electron-electron charge penetration exceeding the nucleus-electron charge penetration. The exchange term ΔE^{ex} and repulsion term ΔE^{rep} between the two H atoms are both zero because exchange interactions only occur between like-spin electrons, and the two 1*s* spin orbitals are already orthonormal to each other due to their opposite spins. When two H atoms form H_2, the 1*s* spin orbitals change shapes to form H_2 molecular spin orbital, resulting in a large polarization energy ΔE^{pol}=−82.35 kcal/mol. Calculated with the CCSD/ACCQ method, which is equivalent to full configuration interaction/ACCQ in this case, the electron correlation energy for H_2 (using HF energy as the reference) is −25.38 kcal/mol.

2. C–H bond in CH_4

A C–H bond in CH_4 was studied and the results are presented in Table I. The geometry of CH_4 was optimized with the MP2/ACCQ method, which leads to a C–H bond length of 1.084 Å. The CH_4 is divided into a CH_3 radical and a H atom, both described with restricted open shell wavefunctions. The ROHF/ACCQ(CP) electrostatic energy ΔE^{ele} is −63.59 kcal/mol. The overlap between the H 1*s* beta spin orbital and the four beta spin orbitals of CH_3 results in −77.47 kcal/mol of exchange energy but simultaneously a strong repulsion energy of 160.66 kcal/mol. Forming a new C–H bond, the orbitals change their shapes significantly and result in a polarization energy of −113.61 kcal/mol. Computed with CCSD(T)/ACCQ(CP), the dispersion energy is −23.83 kcal/mol, and the total interaction energy is −117.83 kcal/mol. Compared to the ROHF method, the RO-B3LYP and RO-BLYP methods produce slightly different ΔE^{ele}: −63.59 for ROHF, −60.41 for RO-B3LYP, and −59.31 for RO-BLYP, all in kcal/mol. Although the ΔE^{ex} and ΔE^{rep} are distinctively different in the DFT and HF methods; their sum shows similarities. The RO-B3LYP and RO-BLYP ΔE^{pol} are ~10 kcal/mol stronger than the HF ones, indicating that KS orbitals are softer than the HF ones. The RO-B3LYP and RO-BLYP ΔE^{disp} and total bond energies are similar to those from the RO-CCSD calculation. Considering preparation energy, zero point energy, and thermal energy, Kass *et al.* obtained 104.2 kcal/mol for the CH_3–H dissociation enthalpy at 298 K.[28]

3. BH_3–CO and BH_3–NH_3

BH_3 forms very strong coordinate covalent bonds with CO and NH_3. Many interaction analyses, most of which have a focus on the charge-transfer interactions, can be found in the literature for these molecules.[9,12,29] Here $BH_3\cdots CO$ and $BH_3\cdots NH_3$ are used as examples to illustrate the role of the polarization energy in the formation of these strong coordinate bonds between main group elements. The MP2/ACCQ optimized B–C distance in $BH_3\cdots CO$ is 1.539 Å, as compared to an experimental value of 1.534±0.01 Å reported by Venkatachar *et al.*[30] The total CCSD(T)/ACCQ(CP) interaction energy between BH_3 and CO is −36.39 kcal/mol, with ΔE^{ele}=−70.53, ΔE^{ex}=−154.02, ΔE^{rep}=+303.20, ΔE^{pol}=−98.63, and ΔE^{disp}=−16.41 kcal/mol (Table I). The MP2/ACCQ optimized B–N distance in $BH_3\cdots NH_3$ is 1.6470 Å, as compared to an experimental value of 1.6576±0.016 Å reported by Thorne *et al.*[31] The total CCSD(T)/ACCQ(CP) interaction energy between BH_3 and NH_3 is −44.42 kcal/mol, with ΔE^{ele}=−82.04, ΔE^{ex}=−123.60, ΔE^{rep}=+238.67, ΔE^{pol}=−68.10, and ΔE^{disp}=−9.35 kcal/mol (Table I). The relatively large ΔE^{pol} values suggest that the orbitals undergo significant change in their shapes, which is typical in the formation of a covalent bond. The bond energy in $BH_3\cdots NH_3$ is stronger than that in $BH_3\cdots CO$ by 8.03 kcal/mol as predicted by the CCSD(T)/ACCQ(CP) calculation. This can be simply explained by the fact that NH_3 has a relatively large dipole while CO has almost no dipole: the ΔE^{elec} in $BH_3\cdots NH_3$ is stronger than that in $BH_3\cdots CO$ by 11.51 kcal/mol. Compared to CCSD(T), MP2 overestimates the bond energies by 0.89 and 2.45 kcal/mol for $BH_3\cdots NH_3$ and $BH_3\cdots CO$. B3LYP and BLYP methods underestimate the bond energy by 2–4 kcal/mol for $BH_3\cdots NH_3$ but overestimate the bond energy by 4–6 kcal/mol for $BH_3\cdots CO$ (Table I). More data for $BH_3\cdots NH_3$ and $BH_3\cdots CO$ can be found in Table S1.[32]

B. Ethane internal rotation barrier

Staggered ethane (*s*-ethane) is lower in energy than eclipsed ethane (*e*-ethane) by ~2.9 kcal/mol. The origin of this energy difference is studied using the EDA method. The geometry of *s*-ethane was optimized with the MP2/ACCQ method, and the geometry of *e*-ethane was obtained from the optimized *s*-ethane by rotating the H–C–C–H dihedral angle from 60° to 0° while holding the internal geometries of the two CH_3 groups and the C–C distance of 1.5211 Å unchanged. EDA calculations were performed with two CH_3 neutral radicals as the monomers. Since the staggered and eclipsed forms are constructed from exactly the same CH_3 groups, their final energy difference can be understood from the CH_3–CH_3 interaction energies.

At the ROHF/ACCQ(CP) level, the CH_3–CH_3 electrostatic interaction ΔE^{ele} in *s*- and *e*-ethane are −147.85 and −148.11 kcal/mol, differing by only 0.26 kcal/mol. The CH_3–CH_3 exchange interactions ΔE^{ex} in *s*- and *e*-ethane are −191.13 and −193.81 kcal/mol, differing by 2.68 kcal/mol due to the more orbital overlap between the CH_3 groups in *e*-ethane. However, the CH_3–CH_3 repulsion interactions ΔE^{rep} in *s*- and *e*-ethane are 400.75 and 406.64 kcal/mol, differing by 5.89 kcal/mol. This is again due to the more orbital overlap between the CH_3 groups in *e*-ethane. The polarization energies ΔE^{pol} for *s*- and *e*-ethane are −148.84 and −148.56 kcal/mol, respectively, differing by only 0.28 kcal/mol. Computed with RO-CCSD/ACCT(CP), the dispersion interaction ΔE^{disp} between the CH_3 groups in *s*- and *e*-ethane are −23.09 and −23.36 kcal/mol, respectively, differing by 0.27 kcal/mol. Using the corrections in ΔE^{disp} obtained from the ROMP2/ACCT(CP) and ROMP2/ACCQ(CP) results (Table S2[32]), the RO-CCSD(T)/

TABLE II. Water cluster interactions (kcal/mol).

Cluster size	Level of theory	ΔE^{ele}	ΔE^{ex}	ΔE^{rep}	ΔE^{pol}	ΔE^{disp}	ΔE
Dimer	CCSD(T)/ACCQ(CP)//MP2/ACCQ	−8.41	−8.85	16.01	−2.38	−1.33	−4.95
	MP2/ACCQ(CP)//MP2/ACCQ	−8.41	−8.85	16.01	−2.38	−1.28	−4.91
	MP2/ACC5(CP)//MP2/ACCQ	−8.41	−8.83	15.99	−2.38	−1.30	−4.92
Trimer	CCSD(T)/ACCT(CP)//MP2/ACCQ	−28.37	−34.48	62.80	−10.69	−4.60	−15.34
	MP2/ACCT(CP)//MP2/ACCQ	−28.37	−34.48	62.80	−10.69	−4.61	−15.35
	MP2/ACCQ(CP)//MP2/ACCQ	−28.39	−34.45	62.74	−10.72	−5.09	−15.90
	MP2/ACC5(CP)//MP2/ACCQ	−28.38	−34.44	62.73	−10.72	−5.15	−15.96
Tetramer	CCSD(T)/ACCT(CP)//MP2/ACCQ	−52.04	−67.16	124.19	−24.97	−7.16	−27.13
	MP2/ACCT(CP)//MP2/ACCQ	−52.04	−67.16	124.19	−24.97	−7.34	−27.31
	MP2/ACCQ(CP)//MP2/ACCQ	−52.03	−67.10	124.09	−25.01	−8.17	−28.22
	MP2/ACC5(CP)//MP2/ACCQ	−52.02	−67.08	124.06	−25.01	−8.27	−28.33

ACCQ(CP) ΔE^{disp} in the *s*- and *e*-ethane are −24.77 and −25.09 kcal/mol, respectively, differing by only 0.32 kcal/mol.

Therefore, from the CH_3-CH_3 interaction point of view, the main reason for *e*-ethane being less stable than *s*-ethane is their difference in the repulsion energy. Attenuated by the changes in the exchange, electrostatic, polarization, and dispersion energies, *e*-ethane is higher in energy by 2.92 kcal/mol than *s*-ethane, in excellent agreement with an experimental value of 2.90 ± 0.03 kcal/mol.[33] Clearly, electrostatic and dispersion interactions favor *e*-ethane, while polarization favors *s*-ethane. These results are consistent with the earlier results obtained by Sovers *et al.* and the recent results obtained by Mo and Gao.[34]

Calculations with ROMP2, UMP2, RO-B3LYP, and RO-BLYP methods lead to essentially the same conclusion, although the two MP2 methods give total interaction energies that are ~7 kcal/mol stronger than those predicted with RO-CCSD and the two DFT methods (Table I). This is simply a fact that for CH_3 radical, which is an open shell system, MP2 predicts less amount of correlation energy than does CCSD, while for the CH_3-CH_3 neutral closed shell molecule, MP2 and CCSD predict more similar correlation energies. Therefore, if the absolute value of the bond energy is of concern, open shell EDA calculations should be performed with CCSD or CCSD(T) methods. For C–H and C–C bonds, B3LYP and BLYP can predict ΔE^{disp} that are in excellent agreement with CCSD.

For comparison, the results of a combined charge and energy decomposition (ETS-NOCV, in the ADF software package) calculation for *s*-ethane performed by Mitoraj *et al.*[15] are $\Delta E_{elstat}=-129.3$, $\Delta E_{Pauli}=+205.9$, and $\Delta E_{orb}=-187.7$, with a $\Delta E_{total}=111.2$ kcal/mol. Although the ETS-NOCV energy decomposition scheme is different from the current EDA scheme, the interaction energy terms show some connections and similarities. For example, their $\Delta E_{elstat}=-129.3$ kcal/mol is close to the $\Delta E^{ele}=-137.30$ kcal/mol from this work, their $\Delta E_{Pauli}=+205.9$ kcal/mol is close to the sum of $\Delta E^{ex}+\Delta E^{rep}=+215.56$ kcal/mol from this work, and their $\Delta E_{orb}=-187.7$ kcal/mol is very close to $\Delta E^{pol}+\Delta E^{disp}=-189.3$ kcal/mol from this work, as shown in Table I by the RO-B3LYP/ACCQ(CP) data. The differences are caused by the differences in the energy decomposition schemes, the differences in the exchange-correlation functionals, and the differences in *s*-ethane geometries and the basis sets.

C. Water dimer, trimer, and tetramer

Water clusters have been studied using quantum chemical methods for a long time.[35,36] Here the results of EDA calculations for water dimer, trimer, and tetramer are presented and discussed (Tables II and III). The geometries of the linear water dimer, the up-up-down cyclic trimer, and the up-down-up-down cyclic tetramer (Fig. 2) were optimized with the MP2/ACCQ method. EDA calculations were performed with the ACCD, ACCT, ACCQ, and ACC5 basis sets. As is well known, the differences between the MP2 and CCSD(T) calculated interaction energies for water clusters are relatively small (<0.2 kcal/mol) due to the cancellation of different types of errors in the MP2 method (Table III and Table S3[32]).

With $\Delta E^{ele}=-8.41$, $\Delta E^{ex}=-8.85$, $\Delta E^{rep}=+16.01$, $\Delta E^{pol}=-2.38$ and $\Delta E^{disp}=-1.33$ kcal/mol, the CCSD(T)/ACCQ(CP)//MP2/ACCQ water dimer interaction energy is −4.95 kcal/mol (Table II), close to the estimated CCSD(T)/complete basis set (CBS) results −5.01 or −5.02 kcal/mol in the literature.[37,38] With $\Delta E^{ele}=-28.38$, $\Delta E^{ex}=-34.44$, $\Delta E^{rep}=+62.73$, $\Delta E^{pol}=-10.72$, and $\Delta E^{disp}=-5.15$ kcal/mol, the MP2/ACC5(CP)//MP2/ACCQ water trimer interaction energy is −15.96 kcal/mol (Table II), close to the estimated MP2/CBS results of −15.80 to −15.82 kcal/mol.[36,39] The CCSD(T)/ACCT(CP) and MP2/ACCT(CP) results are almost identical (Table II), so it is likely that the CCSD(T)/CBS and MP2/CBS results are very similar. Indeed, the estimated MP2/CBS and CCSD(T)/CBS in the literature are −15.80 and −15.82 kcal/mol, almost identical.[39]

With $\Delta E^{ele}=-52.02$, $\Delta E^{ex}=-67.08$, $\Delta E^{rep}=+124.06$, $\Delta E^{pol}=-25.01$, and $\Delta E^{disp}=-8.09$ kcal/mol, the MP2/ACC5(CP)//MP2/ACCQ water tetramer interaction energy is −28.33 kcal/mol (Table II), close to the estimated MP2/CBS result of −27.63 kcal/mol.[36] According to Table II, the CCSD(T)/ACCT(CP) tetramer interaction energy is smaller than the MP2/ACCT(CP) value by 0.18 kcal/mol, so it is likely that the CCSD(T)/CBS value is smaller than the MP2/CBS value by the same amount.

An interesting issue is the pairwise additivity of the interaction terms in many-body systems. As discussed, the

TABLE III. Many-body effects in water tetramer (kcal/mol).

Pair	Level of theory	ΔE^{ele}	ΔE^{ex}	ΔE^{rep}	ΔE^{pol}	ΔE^{disp}	ΔE
Pair 1, 2	MP2/ACC5	−12.24	−16.69	31.00	−4.57	−2.09	−4.59
Pair 1, 3	MP2/ACC5	−1.55	−0.20	0.33	−0.07	−0.20	−1.70
Pair 1, 4	MP2/ACC5	−12.25	−16.71	31.03	−4.57	−2.09	−4.59
Pair 2, 3	MP2/ACC5	−12.19	−16.59	30.81	−4.54	−2.08	−4.60
Pair 2, 4	MP2/ACC5	−1.55	−0.20	0.32	−0.07	−0.20	−1.69
Pair 3, 4	MP2/ACC5	−12.23	−16.68	30.98	−4.57	−2.09	−4.59
Pairwise sum		−52.01	−67.07	124.47	−18.39	−8.75	−21.76
Tetramer 1, 2, 3, 4	MP2/ACC5	−52.01	−67.07	124.05	−25.03	−8.79	−28.85
Many-body effects		0.00	0.00	−0.42	−6.64	−0.04	−7.09
Pair 1, 2	MP2/ACC5(CP)	−12.24	−16.69	31.00	−4.56	−1.96	−4.46
Pair 1, 3	MP2/ACC5(CP)	−1.55	−0.20	0.33	−0.07	−0.18	−1.68
Pair 1, 4	MP2/ACC5(CP)	−12.25	−16.71	31.03	−4.57	−1.96	−4.46
Pair 2, 3	MP2/ACC5(CP)	−12.19	−16.59	30.81	−4.54	−1.95	−4.47
Pair 2, 4	MP2/ACC5(CP)	−1.55	−0.20	0.32	−0.07	−0.18	−1.68
Pair 3, 4	MP2/ACC5(CP)	−12.24	−16.68	30.98	−4.56	−1.96	−4.46
Pairwise sum		−52.02	−67.08	124.47	−18.37	−8.19	−21.21
Tetramer 1, 2, 3, 4	MP2/ACC5(CP)	−52.02	−67.08	124.06	−25.01	−8.27	−28.33
Many-body effects		0.00	0.00	−0.41	−6.64	−0.08	−7.12

electrostatic and exchange terms in the EDA scheme are pairwise additive, while repulsion, polarization, and dispersion are not. EDA calculations were performed for the six pairs of dimers in the water tetramer (Fig. 2) at the MP2/ACC5 level of theory, with and without BSSE corrections (Table III). ACC5 is used because it is almost a CBS for the system so the pairwise additivity under examination is close to that at the CBS limit. As expected, the sums of the pairwise electrostatic and exchange energies in the six dimers are, respectively, the same for the tetramer. For the BSSE uncorrected and corrected cases, the sums of the pairwise dimer repulsion energies are 0.42 and 0.41 kcal/mol more repulsive than that for the actual tetramer and the sums of the dimer dispersion energies are 0.04 and 0.08 kcal/mol less attractive than that for the actual tetramer. So, these two terms, especially the dispersion term, are roughly additive. As expected, the polarization energy is not additive at all: the sum of the dimer polarization energy is 6.64 kcal/mol less attractive than that in the tetramer. Clearly, the total many-body effect (~7.1 kcal/mol) is mainly due to the polarization energy (Table III).

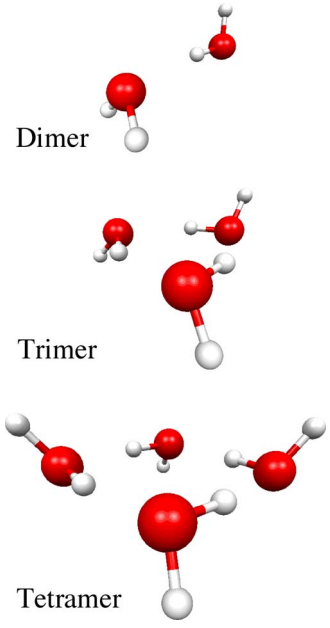

FIG. 2. MP2/ACCQ optimized water dimer, trimer, and tetramer.

D. Nonbonding interaction analysis

The results of EDA calculations for some typical nonbonding interactions are presented in Table IV. These cases are selected because they are often used for comparisons in the literature.

1. He···He

EDA analysis for helium dimer was performed with CCSD(T)/ACC5(CP) at a He–He distance of 2.9634 Å (5.60 bohrs), which is widely used in the literature for comparison. The ΔE^{ele} is −0.0031 kcal/mol, reflecting the fact that there is some orbital overlapping between the two He atoms at this separation. This fact is again shown by some nonzero ΔE^{ex} (−0.0295 kcal/mol) and ΔE^{rep} (+0.0519 kcal/mol). The ΔE^{pol} is only −0.0009 kcal/mol, indicating that the He orbitals do not change much in forming a dimer. As is well known, the main driving force for the formation of a He dimer is the ΔE^{disp}, which is −0.0381 kcal/mol as calculated with CCSD(T)/ACC5(CP). The total CCSD(T)/ACC5(CP) interaction energy is −0.0198 kcal/mol (Table IV), as compared to one of the most accurate results of −0.02186 kcal/mol.[40]

2. Be···Be

EDA analysis was performed for Be dimer at the CCSD(T)/ACC5(CP) level of theory at the experimental Be–Be distance of 2.45 Å.[41] The ΔE^{ele} is −18.56 kcal/mol, indicating that there is a significant orbital overlapping between the two Be atoms. Such an overlap leads to ΔE^{ex}

TABLE IV. Nonbonding interaction (kcal/mol).

Molecule	Level of theory	ΔE^{ele}	ΔE^{ex}	ΔE^{rep}	ΔE^{pol}	ΔE^{disp}	ΔE
He···He	CCSD(T)/ACC5(CP)//2.9634 Å	−0.0031	−0.0295	0.0519	−0.0009	−0.0381	−0.0198
Be···Be	CCSD(T)/ACC5(CP)//2.4500 Å	−18.56	−63.06	110.07	−20.94	−9.45	−1.94
CO_2···CO_2	CCSD(T)/ACCQ(CP)//MP2/ACCQ	−1.76	−2.46	4.31	−0.28	−1.26[a]	−1.45[a]
C_6H_6···H_2O	CCSD(T)/ACCQ(CP)//MP2/ACCT	−3.48	−6.54	11.02	−1.33	−2.83[b]	−3.16[b]
C_6H_6···C_6H_6	CCSD(T)/ACCT(CP)//MP2/ACCD	−3.55	−13.72	22.26	−1.26	−6.05[c]	−2.31[c]
AT	CCSD(T)/ACCQ(CP)//MP2/ACCD	−30.35	−40.21	74.13	−14.02	−6.47[d]	−16.92[d]
GC	CCSD(T)/ACCQ(CP)//MP2/ACCD	−47.95	−52.95	97.47	−22.52	−6.17[e]	−32.12[e]
HF···HF	CCSD(T)/ACC5(CP)//MP2/ACCQ	−6.76	−5.71	10.86	−2.23	−0.72	−4.56
NH_3···H_2O	CCSD(T)/ACCQ(CP)//MP2/ACCQ	−11.88	−14.44	25.95	−4.07	−2.00	−6.44
NH_4^+···H_2O	CCSD(T)/ACCQ(CP)//MP2/ACCQ	−25.38	−18.56	36.80	−11.80	−1.86	−20.79

[a]ΔE^{disp} is the MP2/ACCQ(CP) value corrected by −0.07 kcal/mol from MP2/ACCT(CP) to CCSD(T)/ACCT(CP).
[b]ΔE^{disp} is the MP2/ACCQ(CP) value corrected by +0.33 kcal/mol from MP2/ACCD(CP) to CCSD(T)/ACCD(CP).
[c]ΔE^{disp} is the MP2/ACCT(CP) value corrected by +1.22 kcal/mol from MP2/CCD to CCSD(T)/CCD.
[d]ΔE^{disp} is the MP2/ACCQ(CP) value corrected by +0.21 kcal/mol from MP2/CCD to CCSD(T)/CCD.
[e]ΔE^{disp} is the MP2/ACCQ(CP) value corrected by −0.01 kcal/mol from MP2/CCD to CCSD(T)/CCD.

=−63.06 and ΔE^{rep}=+110.07 kcal/mol. The ΔE^{pol} is −20.94 kcal/mol, indicating that the Be orbitals change their shapes significantly in forming a dimer. As is well known, the main driving force for the formation of a Be dimer is the ΔE^{disp}, which is −9.45 kcal/mol as calculated with CCSD(T)/ACC5(CP). The total interaction is −1.94 kcal/mol (Table IV), as compared to an experimental value of −2.14 to −2.29 kcal/mol.[41] The main difference between the He dimer and Be dimer interactions is caused by the different static and dynamic polarizabilities of the He 1*s* and Be 2*s* orbitals.

3. CO_2···CO_2

The MP2/ACCQ optimized CO_2 dimer shows a parallel displaced shape with a parallel distance of 3.03 Å and a displaced distance of 1.85 Å (Fig. 3), similar to those obtained with the MP2/6-311+G(2*df*) by Tsuzuki *et al.*[42] With ΔE^{ele}=−1.76, ΔE^{ex}=−2.46, ΔE^{rep}=+4.31, ΔE^{pol}=−0.28, and ΔE^{disp}=−1.19 kcal/mol, the total MP2/ACCQ(CP)//MP2/ACCQ interaction energy is −1.38 kcal/mol (Table IV and Table S4[32]), very similar to −1.33 kcal/mol obtained by Tsuzuki *et al.*[42] Since the CCSD(T)/ACCT(CP) interaction energy is 0.07 kcal/mol more negative than the MP2/ACCT(CP) value (Table S4[32]), the CCSD(T)/ACCQ(CP) value can be estimated as −1.45 kcal/mol (Table IV). Bukowski *et al.*[43] performed SAPT calculations for CO_2 dimer but a direct comparison between the SAPT and the current EDA interaction terms is difficult.

4. C_6H_6···H_2O *complex*

An MP2/ACCT optimization of benzene-water complex with no symmetry imposed led to a T-shaped geometry that is very close to a C_s structure (Fig. 3). The distance between the center of mass of benzene and the water oxygen atom is 3.31 Å, comparable to an experimental value of 3.329 Å.[44] The total MP2/ACCQ(CP)//MP2/ACCT interaction energy is −3.49 kcal/mol, with ΔE^{ele}=−3.48, ΔE^{ex}=−6.54, ΔE^{rep}=+11.02, ΔE^{pol}=−1.33, and ΔE^{disp}=−3.16 kcal/mol (Table IV and Table S4[32]). The results from CCSD(T)/ACCD(CP) and MP2/ACCD(CP) suggest that MP2 overestimates the ΔE^{disp} by 0.33 kcal/mol as compared to CCSD(T) (Table S4[32]). Therefore, the CCSD(T)/ACCQ(CP)//MP2/ACCT total interaction energy can be estimated as −3.16 kcal/mol (Table IV), which is very close to a recently estimated CCSD(T)/CBS value of −3.20 kcal/mol.[38]

5. C_6H_6 *dimer*

The distorted T-shaped structure is among the most stable structures for benzene dimer.[45] The distance between the center of mass in the two benzene molecules is 4.69 Å in the MP2/ACCD optimized distorted T-shaped structure (Fig. 3). With ΔE^{ele}=−3.55, ΔE^{ex}=−13.72, ΔE^{rep}=+22.26, ΔE^{pol}=−1.26, and ΔE^{disp}=−7.27 kcal/mol, the total MP2/ACCT(CP)//MP2/ACCD interaction energy for the distorted T-shaped benzene dimer is −3.53 kcal/mol (Table IV and Table S4[32]). CCSD(T)/CCD and MP2/CCD results suggest that compared to CCSD(T), MP2 may overestimate the

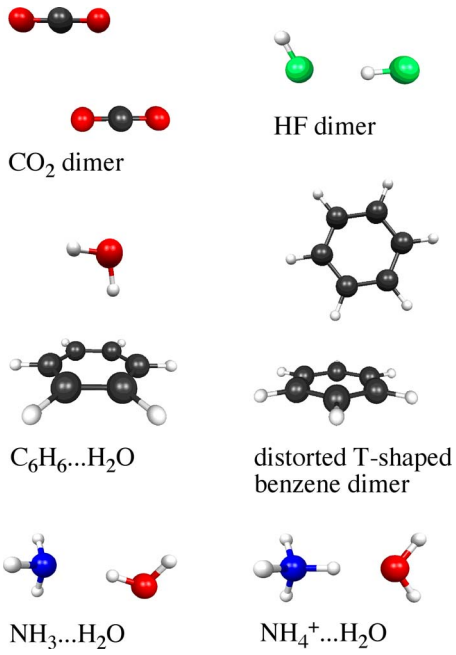

FIG. 3. Nonbonding complexes.

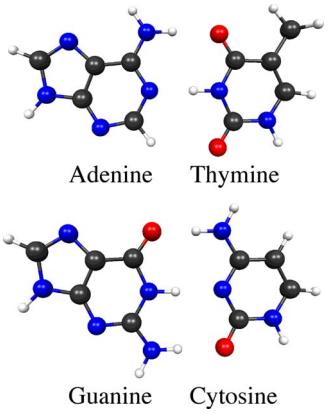

FIG. 4. MP2/ACCD optimized DNA base pairs.

ΔE^{disp} by 1.22 kcal/mol for this benzene dimer (Table S4[32]). Therefore, the CCSD(T)/ACCT(CP) total interaction energy may be estimated as −2.31 kcal/mol (Table IV), as compared to a recently estimated CCSD(T)/CBS value of −2.84 kcal/mol.[38] The relatively large ΔE^{ex} and ΔE^{rep} (−13.72 and +22.26 kcal/mol, respectively) indicate that there is a significant orbital overlap between the two benzene molecules in the dimer. The overlap can also contribute to the ΔE^{ele} as a charge penetration effect. The very small ΔE^{pol} suggests that the benzene orbitals undergo little changes in their shapes in the dimer formation process. As is well known, the main contribution in benzene dimer interaction is the dispersion energy.

6. DNA base pairs

The Watson–Crick structures of the adenine-thymine (AT) and guanine-cytosine (GC) pairs (Fig. 4) were optimized with the MP2/ACCD method in which only the spherical harmonic basis functions were used. The CCSD(T)/CCD calculations were performed with only the spherical harmonic basis functions. The CCSD(T)/CCD dispersion energies are similar to the MP2/CCD ones: −5.91 vs −6.12 kcal/mol for the AT pair and −4.99 vs −4.98 kcal/mol for the GC pair, respectively (Table S4[32]). Therefore, it is likely that CCSD(T) results will be similar to MP2 ones when larger basis sets are used. With ΔE^{ele}=−30.35, ΔE^{ex}=−40.21, ΔE^{rep}=74.13, ΔE^{pol}=−14.02, and ΔE^{disp}=−6.68 kcal/mol, the total MP2/ACCQ(CP)//MP2/ACCD interaction energy for the AT pair is −17.13 kcal/mol (Table IV and Table S4[32]), as compared to −16.6 kcal/mol obtained with resolution of the identity (RI)-MP2/ACCQ//RI-MP2/CCT by Sponer *et al.*[46] Considering the differences between the CCSD(T)/CCD and MP2/CCD results, the CCSD(T)/ACCQ(CP)//MP2/ACCD total interaction energy for the AT pair can be estimated as −16.92 kcal/mol (Table IV). With ΔE^{ele}=−47.95, ΔE^{ex}=−52.95, ΔE^{rep}=97.47, ΔE^{pol}=−22.52, and ΔE^{disp}=−6.16 kcal/mol, the total MP2/ACCQ(CP)//MP2/ACCD interaction energy for the GC pair is −32.11 kcal/mol (Table IV and Table S4[32]), as compared to −31.3 kcal/mol obtained with RI-MP2/ACCQ//RI-MP2/CCT.[46] Considering the differences between the CCSD(T)/CCD and MP2/CCD results, the CCSD(T)/ACCQ(CP)//MP2/ACCD total interaction energy for the GC pair can be estimated as −32.12 kcal/mol (Table IV). The results of an ETS-NOCV energy decomposition calculation performed for the AT pair by Mitoraj *et al.*[15] are ΔE_{elstat}=−31.9, ΔE_{Pauli}=+38.7, and ΔE_{orb}=−22.0, with ΔE_{total}=−15.2 kcal/mol. These values are comparable to the EDA results obtained at the MP2/ACCQ(CP)//MP2/ACCD level of theory: ΔE^{ele}=−30.35, $\Delta E^{ex}+\Delta E^{rep}$=+33.92, and $\Delta E^{pol}+\Delta E^{disp}$=−20.70, with ΔE_{total}=−17.13 kcal/mol. In order to compare to experimentally measured enthalpy changes, preparation energy, zero point energy, and thermal energy are required. This is beyond the scope of the current paper. Experimental $\Delta H_{298\ K}$ values, −12.1 and −21.0 kcal/mol for Watson–Crick AT and GC pairs, respectively, and some discussions can be found in the literature.[47]

7. HF···HF

The MP2/ACCQ optimized F–F distance is 2.744 Å (Fig. 3). The EDA performed at the CCSD(T)/ACC5(CP) level of theory gives ΔE^{ele}=−6.76, ΔE^{ex}=−5.71, ΔE^{rep}=+10.86, ΔE^{pol}=−2.23, and ΔE^{disp}=−0.72 and a total interaction energy of −4.56 kcal/mol (Table IV), which is close to −4.49 kcal/mol obtained with CCSD(T)/ACCQ(CP)//MP2/ACCQ (only the pure harmonic sphere components were used) by Peterson and Dunning.[48] The CCSD(T)/CBS//MP2/ACCQ interaction energy could well be −4.56 kcal/mol. Clearly, all the hydrogen fluoride dimer interaction terms have slightly smaller magnitudes than the corresponding terms for the linear water dimer (Table II).

8. $NH_3\cdots H_2O$

The MP2/ACCQ optimized N–O distance in $NH_3\cdots H_2O$ is 2.921 Å (Fig. 3). The EDA performed at the CCSD(T)/ACCQ(CP) level of theory gives ΔE^{ele}=−11.88, ΔE^{ex}=−14.44, ΔE^{rep}=+25.95, ΔE^{pol}=−4.07, and ΔE^{disp}=−2.00 and a total interaction energy of −6.44 kcal/mol (Table IV), which is similar to an estimated CCSD(T)/CBS//MP2/6-311G** value of −6.36 kcal/mol by Tsuzuki and Luthi.[49] In general, the $NH_3\cdots H_2O$ complex shows a stronger interaction than water dimer and hydrogen fluoride dimer. The relative order of the hydrogen bond strength is $NH_3\cdots H_2O > (H_2O)_2 > (HF)_2$. This can be easily explained by the differences in their ΔE^{ele} terms, which show a reversed order: −11.87 < −8.41 < −6.76 (all in kcal/mol), as calculated from the HF/ACC5 electron densities.

9. $NH_4^+\cdots H_2O$

The MP2/ACCQ optimized N–O distance in $NH_4^+\cdots H_2O$ is 2.698 Å (Fig. 3). At the CCSD(T)/ACCQ(CP) level, EDA shows ΔE^{ele}=−25.38, ΔE^{ex}=−18.56, ΔE^{rep}=+36.80, ΔE^{pol}=−11.80, and ΔE^{disp}=−1.86 and a total interaction energy of −20.79 kcal/mol (Table IV), which is close to an experimental value of −20.6 kcal/mol.[50] Obviously, due to the positive charge on NH_4^+, the magnitudes of the interaction terms in $NH_4^+\cdots H_2O$ are all larger than those in $NH_3\cdots H_2O$ except for the dispersion term. The large ΔE^{pol} in $NH_4^+\cdots H_2O$ indicates that the H_2O orbitals undergo significant changes in their shapes in order to maximize the strength of the hydrogen bond.

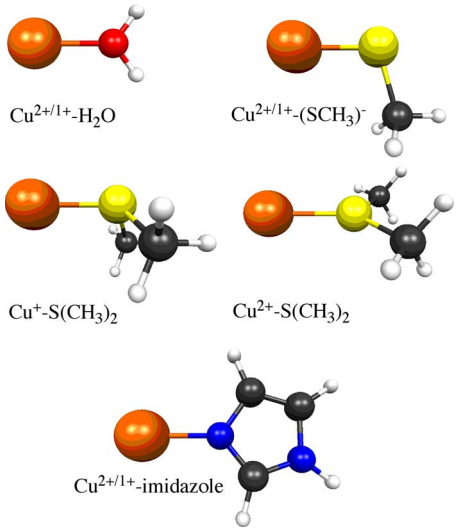

FIG. 5. MP2/ACCT optimized $Cu^{2+/1+}$ complexes.

E. Cu-ligand interaction

Being an essential element, Cu plays an important role in living systems. The interaction energies between Cu ions and some biologically interesting ligands have been measured experimentally and calculated with quantum chemical methods.[51] An interaction analysis with the RVS method was performed by Gresh *et al.* for some typical Cu^+ complexes,[52] but a similar analysis has not been done for Cu^{2+} complexes. In this work the interactions in $Cu-H_2O$, Cu-imidazole, $Cu-(SCH_3)^-$, and $Cu-S(CH_3)$ complexes (Fig. 5) are studied.

All the geometries were optimized with the MP2/ACCT method. EDA calculations were performed with CCSD, CCSD(T), MP2, B3LYP, and BLYP methods based on the MP2/ACCT optimized geometries. In principle, the geometries should be optimized using the same method for the EDA calculations, especially when distinctively different methods such as MP2 and DFT are used (the basis set effects are usually not problematic in the ACC*n* series). A test on the $Cu^{2+}-H_2O$ complex shows that the geometries optimized with the U-B3LYP/ACCT and UMP2/ACCT methods are similar, and the subsequent EDA calculations using the U-B3LYP/ACCT method show very similar total interaction energies (differ by ~1 kcal/mol, Table S5[32]) with differences mainly in the Heitler–London term (i.e., $\Delta E^{ele}+\Delta E^{ex}+\Delta E^{rep}$). The CP method was used to correct the BSSE, but approximately half of the cases did not converge either in the HF-SCF, DFT-SCF, or CCSD stage. Therefore, in Table V only the BSSE uncorrected data are presented for consistence and comparison. Using ACCQ, the BSSE corrected and uncorrected results are similar to within 0.5 kcal/mol for almost all the cases available for comparison. More data can be found in Table S5.[32]

The MP2/ACCT optimized Cu^+-H_2O and $Cu^{2+}-H_2O$ complexes show similar planar C_{2v} geometries with Cu–O distances of 1.918 and 1.820 Å, respectively (Fig. 5). With $\Delta E^{ele}=-58.21$, $\Delta E^{ex}=-41.25$, $\Delta E^{rep}=89.67$, $\Delta E^{pol}=-19.39$, and $\Delta E^{disp}=-9.97$ kcal/mol, the total CCSD(T)/ACCQ interaction energy in Cu^+-H_2O is -39.14 kcal/mol (Table V). The relatively small ΔE^{pol} and large ΔE^{ele} suggest that the Cu^+-H_2O interaction is mainly electrostatic. With $\Delta E^{ele}=-96.46$, $\Delta E^{ex}=-40.29$, $\Delta E^{rep}=+104.16$, $\Delta E^{pol}=-63.89$, and $\Delta E^{disp}=-10.48$ kcal/mol, the total UMP2/ACCQ interaction energy in $Cu^{2+}-H_2O$ is -106.96 kcal/mol (Table V), much larger than that in Cu^+-H_2O. If only the depletion of an electron on going from Cu^+ to Cu^{2+} is considered, the magnitude of the ΔE^{ex} should decrease. However, a shorter distance in $Cu^{2+}-H_2O$ brings the ΔE^{ex} back to -40.29 kcal/mol, similar to -41.25 kcal/mol in Cu^+-H_2O. The shorter distance in $Cu^{2+}-H_2O$ also results in a sizable increase in the ΔE^{rep}. The large ΔE^{pol} suggests that the $Cu^{2+}-H_2O$ has a large covalency component. For Cu^+-H_2O, MP2, B3LYP, and BLYP overestimate the total interaction energy by ~1, ~2, and ~4 kcal/mol as compared to CCSD(T). For $Cu^{2+}-H_2O$, RO-MP2, UMP2, U-B3LYP, and U-BLYP overestimate the total interaction energy by ~0, ~0, ~11, and ~25 kcal/mol as compared to RO-CCSD (Table V). A CCSD(T) calculation[53] in the literature shows that the $Cu^{2+}-H_2O$ distance is 1.841 Å, and the interaction energy is -107.7 kcal/mol, close to the CCSD result of -106.96 from this work. The main reason for the overestimation is the polarization energy, which is -63.95 kcal/mol for ROMP2, -63.89 kcal/mol for UMP2, -82.81 kcal/mol for U-B3LYP, and -105.59 kcal/mol for U-BLYP.

The MP2/ACCT optimized Cu^+-imidazole and Cu^{2+}-imidazole complexes show similar C_s planar geometries with Cu–N distances of 1.864 and 1.806 Å, respectively (Fig. 5). The total MP2/ACCQ interaction energy in Cu^+-imidazole is -73.92 kcal/mol, with $\Delta E^{ele}=-109.52$, $\Delta E^{ex}=-72.39$, $\Delta E^{rep}=+165.87$, $\Delta E^{pol}=-35.62$, and $\Delta E^{disp}=-22.26$ kcal/mol (Table V). The electrostatic energy has the largest contribution. In Cu^{2+}-imidazole the total ROMP2/ACCQ interaction energy is -247.62 kcal/mol, with $\Delta E^{ele}=-117.25$, $\Delta E^{ex}=-37.75$, $\Delta E^{rep}=+97.22$, $\Delta E^{pol}=-128.94$, and $\Delta E^{disp}=-60.99$ kcal/mol (Table V). The electrostatic energy has the largest contribution, but polarization energy is also significant. Due to the large polarization energy, the coordinate bond of Cu^{2+}-imidazole should be considered as a covalent bond. For Cu^+-imidazole, MP2, B3LYP, and BLYP overestimate the interaction energy by ~3, ~4, and ~9 kcal/mol as compared to CCSD(T). For Cu^{2+}-imidazole, ROMP2, RO-B3LYP, and RO-BLYP overestimate the total interaction energy by ~19, ~18, and ~34 kcal/mol as compared to the RO-CCSD method.

The MP2/ACCT optimized $Cu^+-(SCH_3)^-$ and $Cu^{2+}-(SCH_3)^-$ complexes show similar geometries with Cu–S distances of 2.077 and 2.146 Å, respectively (Fig. 5). Though the $Cu^{2+}-S$ interaction is stronger, their distance is slightly longer. The total MP2/ACCQ interaction energy in $Cu^+-(SCH_3)^-$ is -195.17 kcal/mol, with $\Delta E^{ele}=-256.89$, $\Delta E^{ex}=-98.09$, $\Delta E^{rep}=+239.18$, $\Delta E^{pol}=-45.61$, and $\Delta E^{disp}=-33.77$ kcal/mol. The electrostatic energy makes the main contribution. The $Cu^+-(SCH_3)^-$ bond is more covalent than that of Cu^+-H_2O but less covalent than the typical BH_3-CO and BH_3-NH_3 coordinate bonds (Table I). The total UMP2/ACCQ energy in $Cu^{2+}-(SCH_3)^-$ is -493.29 kcal/mol, with $\Delta E^{ele}=-371.97$, $\Delta E^{ex}=-64.28$, $\Delta E^{rep}=+181.18$, $\Delta E^{pol}=-158.94$, and $\Delta E^{disp}=-79.28$ kcal/mol. The magnitudes of

TABLE V. Cu-ligand interaction (kcal/mol).

Molecule	Level of theory	ΔE^{ele}	ΔE^{ex}	ΔE^{rep}	ΔE^{pol}	ΔE^{disp}	ΔE
Cu^+-H_2O	CCSD(T)/ACCQ//MP2/ACCT	−58.21	−41.25	89.67	−19.39	−9.97	−39.14
	MP2/ACCQ//MP2/ACCT	−58.21	−41.25	89.67	−19.39	−11.00	−40.18
	B3LYP/ACCQ//MP2/ACCT	−61.14	−23.68	79.68	−29.25	−6.84	−41.23
	BLYP/ACCQ//MP2/ACCT	−62.17	−17.26	77.08	−32.95	−7.89	−43.19
Cu^+-imidazole	CCSD(T)/ACCT//MP2/ACCT	−109.97	−72.67	166.68	−35.82	−19.05	−70.83
	MP2/ACCT//MP2/ACCT	−109.97	−72.67	166.68	−35.82	−21.98	−73.76
	MP2/ACCQ//MP2/ACCT	−109.52	−72.39	165.87	−35.62	−22.26	−73.92
	B3LYP/ACCQ//MP2/ACCT	−114.08	−41.50	141.77	−52.48	−8.13	−74.42
	BLYP/ACCQ//MP2/ACCT	−116.03	−31.60	136.25	−58.81	−9.33	−79.53
$Cu^+-(SCH_3)^-$	CCSD(T)/ACCQ//MP2/ACCT	−256.89	−98.09	239.18	−45.61	−30.11	−191.51
	MP2/ACCQ//MP2/ACCT	−256.89	−98.09	239.18	−45.61	−33.77	−195.17
	B3LYP/ACCQ//MP2/ACCT	−257.43	−58.67	199.78	−71.43	−10.78	−198.52
	BLYP/ACCQ//MP2/ACCT	−257.96	−46.95	190.97	−81.21	−12.27	−207.41
$Cu^+-S(CH_3)_2$	CCSD(T)/ACCT//MP2/ACCT	−89.77	−66.54	156.27	−35.30	−20.73	−56.08
	MP2/ACCT//MP2/ACCT	−89.77	−66.54	156.27	−35.30	−23.92	−59.26
	MP2/ACCQ//MP2/ACCT	−89.34	−66.35	155.61	−35.20	−24.42	−59.70
	B3LYP/ACCQ//MP2/ACCT	−89.44	−38.62	129.25	−54.62	−8.20	−61.62
	BLYP/ACCQ//MP2/ACCT	−90.87	−30.15	124.22	−62.00	−9.46	−68.26
$Cu^{2+}-H_2O$	RO-CCSD/ACCT//UMP2/ACCT	−96.58	−40.33	104.51	−63.95	−10.43	−106.78
	ROMP2/ACCT//UMP2/ACCT	−96.58	−40.33	104.51	−63.95	−10.04	−106.40
	UMP2/ACCQ//UMP2/ACCT	−96.46	−40.29	104.16	−63.89	−10.48	−106.96
	U-B3LYP/ACCQ//UMP2/ACCT	−94.46	−21.90	91.81	−82.81	−10.35	−117.70
	U-BLYP/ACCQ//UMP2/ACCT	−87.62	−14.95	89.18	−105.59	−12.74	−131.71
Cu^{2+}-imidazole	RO-CCSD/ACCD-T[a]//ROMP2/ACCT	−118.94	−37.88	97.74	−127.69	−47.58	−234.35
	ROMP2/ACCD-T[a]//ROMP2/ACCT	−118.94	−37.88	97.74	−127.69	−66.64	−253.41
	ROMP2/ACCQ//ROMP2/ACCT	−117.25	−37.75	97.22	−128.94	−60.99	−247.62
	RO-B3LYP/ACCQ//ROMP2/ACCT	−117.59	−21.56	85.17	−180.31	−12.42	−246.72
	RO-BLYP/ACCQ//ROMP2/ACCT	−93.16	−34.28	81.35	−203.26	−13.20	−262.54
$Cu^{2+}-(SCH_3)^-$	RO-CCSD/ACCD-T[b]//UMP2/ACCT	−375.94	−66.69	187.42	−156.79	−61.53	−473.53
	ROMP2/ACCD-T[b]//UMP2/ACCT	−375.94	−66.69	187.42	−156.79	−87.65	−499.65
	UMP2/ACCD-T[b]//UMP2/ACCT	−375.40	−64.72	184.30	−157.31	−84.46	−497.59
	UMP2/ACCQ//UMP2/ACCT	−371.97	−64.28	181.18	−158.94	−79.28	−493.29
	U-B3LYP/ACCQ//UMP2/ACCT	−366.99	−39.36	155.99	−227.39	−16.43	−494.18
	U-BLYP/ACCQ//UMP2/ACCT	−353.56	−30.96	142.55	−254.59	−17.87	−514.43
$Cu^{2+}-S(CH_3)_2$	RO-CCSD/ACCD-T[b]//UMP2/ACCT	−57.84	−20.54	54.20	−119.27	−52.49	−195.92
	ROMP2/ACCD-T[b]//UMP2/ACCT	−57.84	−20.54	54.20	−119.27	−77.61	−221.04
	UMP2/ACCD-T[b]//UMP2/ACCT	−57.83	−20.53	54.19	−120.61	−74.16	−218.94
	UMP2/ACCQ//UMP2/ACCT	−57.16	−19.90	52.57	−120.93	−69.49	−214.90
	U-B3LYP/ACCQ//UMP2/ACCT	−53.34	−11.69	46.58	−187.50	−11.22	−217.18
	U-BLYP/ACCQ//UMP2/ACCT	−45.36	−10.78	44.91	−212.90	−12.39	−236.53

[a]Mixed basis set: ACCT for Cu, ACCD for the three C, N, and C atoms closest to Cu, and CCD for other atoms.
[b]Mixed basis set: ACCT for Cu and ACCD for other atoms.

the exchange and repulsion energies in $Cu^{2+}-(SCH_3)^-$ are ~2/3 of those in $Cu^+-SCH_3^-$ due to the increase in the Cu–S distance and the loss of an electron. It is well known that Cu^{2+}-thiolate bond is highly covalent.[54] The large polarization energy from EDA is in accord with the established picture. For $Cu^+-(SCH_3)^-$, MP2, B3LYP, and BLYP overestimate the total interaction energy by ~4, ~7, and ~16 kcal/mol as compared to CCSD(T). For $Cu^{2+}-(SCH_3)^-$, UMP2, U-B3LYP, and U-BLYP overestimate the interaction energy by ~24, ~25, and ~45 kcal/mol as compared to RO-CCSD.

$Cu^+-S(CH_3)_2$ and $Cu^{2+}-S(CH_3)_2$ show completely different structures (Fig. 5). Although Cu^{2+} has a stronger interaction with $S(CH_3)_2$, the $Cu^{2+}-S$ distance, 2.341 Å, is actually longer than the Cu^+-S distance of 2.159 Å. For $Cu^+-S(CH_3)_2$, the MP2/ACCQ total interaction energy is −59.70 kcal/mol, with $\Delta E^{ele}=-89.34$, $\Delta E^{ex}=-66.35$, $\Delta E^{rep}=+155.61$, $\Delta E^{pol}=-35.20$, and $\Delta E^{disp}=-24.42$ kcal/mol. For $Cu^{2+}-S(CH_3)_2$, the UMP2/ACCQ total interaction energy is −214.90 kcal/mol, with $\Delta E^{ele}=-57.16$, $\Delta E^{ex}=-19.90$, $\Delta E^{rep}=+52.57$, $\Delta E^{pol}=-120.93$, and $\Delta E^{disp}=-69.49$ kcal/mol. Clearly, the $Cu^+-S(CH_3)_2$ interaction is dominated by electrostatic, while the $Cu^{2+}-S(CH_3)_2$ interaction is dominated by polarization, like a covalent bond. For $Cu^+-S(CH_3)_2$, MP2, B3LYP, and BLYP overestimate the total interaction energy by ~3, ~5, and ~12 kcal/mol as compared to CCSD(T). For $Cu^{2+}-S(CH_3)_2$, UMP2, U-B3LYP, and U-BLYP overestimate the interaction energy by ~23, ~25, and ~45 kcal/mol as compared to the RO-CCSD method.

To summarize, the negatively charged thiolate $(SCH_3)^-$ forms the strongest bond to $Cu^{2+/1+}$. The neutral ligands imi-

TABLE VI. Ionic interaction (kcal/mol).

Molecule	Level of theory	ΔE^{ele}	ΔE^{ex}	ΔE^{rep}	ΔE^{pol}	ΔE^{disp}	ΔE
Li^+F^-	CCSD(T)/ACC5(CP)//MP2/ACCQ	−206.29	−21.71	63.39	−21.98	+2.34	−184.25
Li^+Cl^-	CCSD(T)/ACC5(CP)//MP2/ACCQ	−157.97	−15.43	46.85	−25.82	−1.29	−153.66
Na^+F^-	CCSD(T)/ACC5(CP)//MP2/ACCQ	−176.30	−21.40	52.61	−9.06	+0.66	−153.49
Na^+Cl^-	CCSD(T)/ACC5(CP)//MP2/ACCQ	−143.89	−17.99	45.14	−12.92	−2.21	−131.87

dazole and $S(CH_3)$ form much weaker coordinate bonds to $Cu^{2+/1+}$. Water forms the weakest coordinate bond to $Cu^{2+/1+}$. Cu^+-ligand interactions are mainly electrostatic, while Cu^{2+}-ligand interactions are much more covalent. MP2, B3LYP, and BLYP can predict reasonably good binding energies for Cu^+ complexes.

F. Ionic bonding

There is no doubt that electron correlation methods such as MP2 and CCSD(T) will give a lower total energy as compared to HF methods for any molecular system with more than one electron. For intermolecular interactions, however, electron correlation methods do not necessarily predict stronger interaction energies than HF methods, as have been documented, for example, by Sannigrahi *et al.* in a quantum chemical study of alkali halides.[55] Here the results of EDA calculations for Li^+F^-, Li^+Cl^-, Na^+F^-, and Na^+Cl^- are reported. Because Li^+ and Na^+ ions have no valence electrons, the MP2 and CCSD(T) calculations discussed below were performed with full excitation (no frozen core).

The MP2/ACCQ optimized bond lengths of Li^+F^-, Li^+Cl^-, Na^+F^-, and Na^+Cl^- are 1.574, 2.023, 1.949, and 2.380 Å, respectively, compared well to the experimental values of 1.564, 2.021, 1.926, and 2.361 Å.[27] The total CCSD(T)/ACC5(CP)//MP2/ACCQ interaction energies of these four ionic complexes are −184.25, −153.66, −153.49, and −131.87 kcal/mol, respectively (Table VI), in excellent agreement with the experimental values of -183.5 ± 2.2, -154.0 ± 0.1, -153.3 ± 0.9, and -132.4 ± 0.8 kcal/mol.[56] Clearly, the ions form strong ionic bonds as indicated by the ΔE^{ele} values of −206.29, −157.97, −176.30, and −143.88 kcal/mol. The relatively small polarization energies are mainly from the anions F^- and Cl^- as the Li^+ and Na^+ cations are typical hard ions. As expected, Li^+Cl^- shows the largest polarization energy of −25.82 kcal/mol, while Na^+F^- shows the smallest polarization energy of −9.06 kcal/mol (Table VI). The ΔE^{ex} and E^{rep} are similar in all of these ion pairs.

It is interesting that the CCSD(T)/ACC5(CP) dispersion energies in Li^+F^- and Na^+F^- are positive (repulsive): +2.34 and +0.66 kcal/mol, respectively. Similar values can be found in an earlier work that used HF and MP2 methods.[55] This is caused by the differences in the intra- and interionic correlation energy on going from noninteracting to interacting ions and can be basis set and distance sensitive (Table S6[32]). It is obvious that at the CBS limit, CCSD(T) will predict a positive dispersion energy for Li^+F^-, but the sign for Na^+F^- is not clear. A plot of the ΔE^{disp} obtained with CCSD(T)/ACCQ(CP) for Li^+F^- at different separation distances shows that the ΔE^{disp} will turn into negative (attractive) at 2.09 Å (Fig. 6).

V. CONCLUSION

An EDA method was implemented in GAMESS to perform interaction analysis for both bonding and nonbonding interactions on the basis of RHF, ROHF, UHF, R-KS, RO-KS, and U-KS wavefunctions. For HF methods, MP2, CCSD, and CCSD(T) are used to evaluate the dispersion energy. To conclude, the following points are highlighted:

(1) This EDA is basis set insensitive because no charge-transfer term or assignment of electron density to monomers is involved. The interaction terms show convergence as the basis set approaches the CBS limit. For most of the tested cases, the ACCT basis set converges the HF and DFT interaction terms, and the ACCQ basis set with BSSE correction converges the MP2, CCSD, and CCSD(T) dispersion terms, respectively, to within 1.0 kcal/mol of the CBS limit (see the data in supplementary tables).

(2) Covalent bonds are characterized by large polarization energies, typically −100 kcal/mol, as the results of significant orbital deformations. B3LYP and BLYP methods can predict bond energies that are comparable to those from the CCSD method for some typical covalent bonds such as H–H, C–H, and C–C (Table I), but the errors for coordinate covalent bonds are substantially large (Tables I and V).

(3) The results for staggered and eclipsed ethane clearly indicate that the exchange-repulsion energy is the main cause of the ~3 kcal/mol rotation barrier (Table I).

(4) For water tetramer, many-body polarization is −6.64 kcal/mol, many-body repulsion is −0.41 kcal/mol, and many-body dispersion is −0.08 kcal/mol, as computed with the MP2/ACC5 method (Table III).

(5) The interaction energies for two DNA base pairs, AT and GC, are obtained as −17.13 and −32.11 kcal/mol

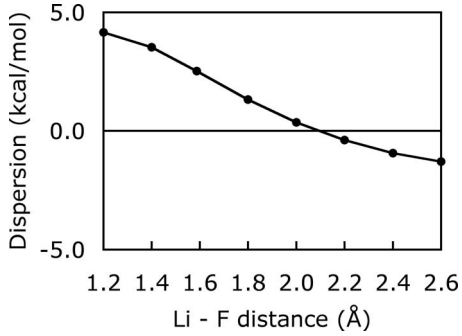

FIG. 6. Positive dispersion interaction between Li^+ and F^- calculated with CCSD(T)/ACCQ(CP). The experimental Li–F equilibrium distance is 1.564 Å.

at the MP2/ACCQ(CP)//MP2/ACCD levels of theory (Table IV).

(6) Cu^+-H_2O, Cu^+-imidazole, $Cu^+-(SCH_3)^-$, and $Cu^+-S(CH_3)_2$ interactions are mainly electrostatic, while $Cu^{2+}-H_2O$, Cu^{2+}-imidazole, $Cu^{2+}-(SCH_3)^-$, and $Cu^{2+}-S(CH_3)_2$ interactions are covalent. Compared to CCSD, MP2, B3LYP, and BLYP tend to overestimate Cu-ligand interactions, especially for Cu^{2+} complexes (Table V).

(7) For Li^+F^-, CCSD(T) predicts smaller interaction energy than the HF method (Table VI).

ACKNOWLEDGMENTS

This work was supported by startup funds from the University of Nebraska-Lincoln. The authors are grateful to Michael W. Schmidt for his critical comments on the manuscript.

[1] A. J. Stone, *The Theory of Intermolecular Forces* (Oxford University Press, New York, 1996).
[2] K. Szalewicz and B. Jeziorski, Mol. Phys. **38**, 191 (1979); B. Jeziorski, R. Moszynski, and K. Szalewicz, Chem. Rev. (Washington, D.C.) **94**, 1887 (1994).
[3] A. J. Misquitta, R. Podeszwa, B. Jeziorski, and K. Szalewicz, J. Chem. Phys. **123**, 214103 (2005); H. L. Williams and C. F. Chabalowski, J. Phys. Chem. A **105**, 646 (2001); G. Jansen and A. Hesselmann, *ibid.* **105**, 11156 (2001); A. Heßelmann and G. Jansen, Chem. Phys. Lett. **357**, 464 (2002).
[4] G. Chalasinski and M. M. Szczesniak, Mol. Phys. **63**, 205 (1988).
[5] V. F. Lotrich and K. Szalewicz, J. Chem. Phys. **106**, 9688 (1997); V. F. Lotrich, P. Jankowski, and K. Szalewicz, *ibid.* **108**, 4725 (1998).
[6] K. Morokuma, J. Chem. Phys. **55**, 1236 (1971); K. Morokuma and K. Kitaura, in *Chemical Applications of Atomic and Molecular Electronic Potentials*, edited by P. Politzer and D. G. Truhlar (Plenum, New York, 1981), p. 215.
[7] K. Kitaura and K. Morokuma, Int. J. Quantum Chem. **10**, 325 (1976).
[8] W. Chen and M. S. Gordon, J. Phys. Chem. **100**, 14316 (1996).
[9] E. D. Glendening and A. Streitwieser, J. Chem. Phys. **100**, 2900 (1994).
[10] P. S. Bagus, K. Hermann, and J. C. W. Bauschlicher, J. Chem. Phys. **80**, 4378 (1984); P. S. Bagus and F. Illas, *ibid.* **96**, 8962 (1992).
[11] W. J. Stevens and W. H. Fink, Chem. Phys. Lett. **139**, 15 (1987).
[12] Y. R. Mo, J. L. Gao, and S. D. Peyerimhoff, J. Chem. Phys. **112**, 5530 (2000).
[13] R. Z. Khaliullin, E. A. Cobar, R. C. Lochan, A. T. Bell, and M. Head-Gordon, J. Phys. Chem. A **111**, 8753 (2007).
[14] T. Ziegler and A. Rauk, Theor. Chem. Acc. **46**, 1 (1977); G. T. te Velde, F. M. Bickelhaupt, E. J. Baerends, C. F. Guerra, S. J. A. Van Gisbergen, J. G. Snijders, and T. Ziegler, J. Comput. Chem. **22**, 931 (2001); F. M. Bickelhaupt and E. J. Baerends, *Reviews in Computational Chemistry* (Wiley-VCH, New York, 2000), Vol. 15, p. 1.
[15] M. P. Mitoraj, A. Michalak, and T. Ziegler, J. Comput. Chem. **5**, 962 (2009).
[16] E. D. Glendening, J. Phys. Chem. A **109**, 11936 (2005); P. Reinhardt, J. P. Piquemal, and A. Savin, J. Chem. Theory Comput. **4**, 2020 (2008).
[17] T. Ziegler and A. Rauk, Inorg. Chem. **18**, 1755 (1979).
[18] I. C. Hayes and A. J. Stone, Mol. Phys. **53**, 83 (1984).
[19] M. W. Schmidt, K. K. Baldridge, J. A. Boatz, S. T. Elbert, M. S. Gordon, J. H. Jensen, S. Koseki, N. Matsunaga, K. A. Nguyen, S. J. Su, T. L. Windus, M. Dupuis, and J. A. Montgomery, J. Comput. Chem. **14**, 1347 (1993); M. S. Gordon and M. W. Schmidt, in *Theory and Applications of Computational Chemistry*, edited by C. E. Dykstra, G. Frenking, K. S. Kim, and G. E. Scuseria (Elsevier, Amsterdam, 2005).
[20] J. A. P. J. S. Binkley, Int. J. Quantum Chem. **9**, 229 (1975); M. J. Frisch, M. Head-Gordon, and J. A. Pople, Chem. Phys. Lett. **166**, 275 (1990); C. M. Aikens, S. P. Webb, R. L. Bell, G. D. Fletcher, M. W. Schmidt, and M. S. Gordon, Theor. Chem. Acc. **110**, 233 (2003).
[21] P. Piecuch, S. A. Kucharski, K. Kowalski, and M. Musial, Comput. Phys. Commun. **149**, 71 (2002); J. L. Bentz, R. M. Olson, M. S. Gordon, M. W. Schmidt, and R. A. Kendall, *ibid.* **176**, 589 (2007); R. M. Olson, J. L. Bentz, R. A. Kendall, M. W. Schmidt, and M. S. Gordon, J. Chem. Theory Comput. **3**, 1312 (2007); P. Piecuch and M. Wloch, J. Chem. Phys. **123**, 224105 (2005); M. Wloch, J. R. Gour, and P. Piecuch, J. Phys. Chem. A **111**, 11359 (2007).
[22] G. D. Fletcher, M. W. Schmidt, B. M. Bode, and M. S. Gordon, Comput. Phys. Commun. **128**, 190 (2000).
[23] S. F. Boys and F. Bernardi, Mol. Phys. **19**, 553 (1970).
[24] T. H. Dunning, J. Chem. Phys. **90**, 1007 (1989); N. B. Balabanov and K. A. Peterson, *ibid.* **123**, 064107 (2005).
[25] R. H. Hertwig and W. Koch, Chem. Phys. Lett. **268**, 345 (1997).
[26] A. D. Becke, Phys. Rev. A **38**, 3098 (1988); C. Lee, W. Yang, and R. G. Parr, Phys. Rev. B **37**, 785 (1988).
[27] K. P. Huber and G. Herzberg, *Molecular Spectra and Molecular Structure IV. Constants of Diatomic Molecules* (Van Nostrand Reinhold, New York, 1979).
[28] Z. X. Tian, A. Fattahi, L. Lis, and S. R. Kass, J. Am. Chem. Soc. **128**, 17087 (2006).
[29] V. Jonas, G. Frenking, and M. T. Reetz, J. Am. Chem. Soc. **116**, 8741 (1994); K. Morokuma, Acc. Chem. Res. **10**, 294 (1977); Y. R. Mo, L. C. Song, W. Wu, and Q. N. Zhang, J. Am. Chem. Soc. **126**, 3974 (2004).
[30] A. C. Venkatachar, R. C. Taylor, and R. L. Kuczkowski, J. Mol. Struct. **38**, 17 (1977).
[31] L. R. Thorne, R. D. Suenram, and F. J. Lovas, J. Chem. Phys. **78**, 167 (1983).
[32] See EPAPS Document No. http://dx.doi.org/10.1063/1.3159673 for Tables S1–S6.
[33] S. Weiss and G. E. Leroi, J. Chem. Phys. **48**, 962 (1968); E. Hirota, S. Saito, and Y. Endo, *ibid.* **71**, 1183 (1979).
[34] O. J. Sovers, C. W. Kern, R. M. Pitzer, and M. Karplus, J. Chem. Phys. **49**, 2592 (1968); Y. R. Mo and J. L. Gao, Acc. Chem. Res. **40**, 113 (2007).
[35] S. Scheiner, Annu. Rev. Phys. Chem. **45**, 23 (1994).
[36] S. S. Xantheas, C. J. Burnham, and R. J. Harrison, J. Chem. Phys. **116**, 1493 (2002).
[37] W. Klopper, J. van Duijneveldt-van de Rijdt, and F. B. van Duijneveldt, Phys. Chem. Chem. Phys. **2**, 2227 (2000).
[38] S. K. Min, E. C. Lee, H. M. Lee, D. Y. Kim, D. Kim, and K. S. Kim, J. Comput. Chem. **29**, 1208 (2008).
[39] J. A. Anderson, K. Crager, L. Fedoroff, and G. S. Tschumper, J. Chem. Phys. **121**, 11023 (2004).
[40] J. B. Anderson, J. Chem. Phys. **120**, 9886 (2004).
[41] V. E. Bondybey and J. H. English, J. Chem. Phys. **80**, 568 (1984).
[42] S. Tsuzuki, T. Uchimaru, M. Mikami, and K. Tanabe, J. Chem. Phys. **109**, 2169 (1998).
[43] R. Bukowski, J. Sadlej, B. Jeziorski, P. Jankowski, and K. Szalewicz, J. Chem. Phys. **110**, 3785 (1999).
[44] H. S. Gutowsky, T. Emilsson, and E. Arunan, J. Chem. Phys. **99**, 4883 (1993).
[45] R. A. DiStasio, Jr., G. von Helden, R. P. Steele, and M. Head-Gordon, Chem. Phys. Lett. **437**, 277 (2007).
[46] J. Sponer, P. Jurecka, and P. Hobza, J. Am. Chem. Soc. **126**, 10142 (2004).
[47] A. B. T. I. K. Yanson and L. F. Sukhodub, Biopolymers **18**, 1149 (1979); C. Fonseca Guerra, F. M. Bickelhaupt, J. G. Snijders, and E. J. Baerends, J. Am. Chem. Soc. **122**, 4117 (2000); J. Sponer, J. Leszczynski, and P. Hobza, J. Phys. Chem. **100**, 1965 (1996).
[48] K. A. Peterson and J. T. H. Dunning, J. Chem. Phys. **102**, 2032 (1995).
[49] S. Tsuzuki and H. P. Luthi, J. Chem. Phys. **114**, 3949 (2001).
[50] M. Meot-Ner and C. V. Speller, J. Phys. Chem. **90**, 6616 (1986).
[51] S. Hoyau and G. Ohanessian, Chem. Phys. Lett. **280**, 266 (1997); J. Am. Chem. Soc. **119**, 2016 (1997).
[52] N. Gresh, C. Policar, and C. Giessner-Prettre, J. Phys. Chem. A **106**, 5660 (2002).
[53] J. Poater, M. Sola, A. Rimola, L. Rodriguez-Santiago, and M. Sodupe, J. Phys. Chem. A **108**, 6072 (2004).
[54] E. I. Solomon, S. I. Gorelsky, and A. Dey, J. Comput. Chem. **27**, 1415 (2006).
[55] A. B. Sannigrahi, P. K. Nandi, and P. V. Schleyer, J. Am. Chem. Soc. **116**, 7225 (1994).
[56] *JANAF Thermochemical Tables, 3rd Ed.*, edited by M. W. Chase, Jr., C. A. Davies, J. R. Davies, Jr., D. J. Fulrip, R. A. McDonald, and A. N. Syverud, J. Phys. Chem. Ref. Data **14**, Supplement 1, 1985.